Supplementary Information for

Switchable Chirality of Circularly Polarized Luminescence in Dilute Solution Based on the Solvent-dependent Helix Inversion of Poly(quinoxaline-2,3-diyl)s

Yuuya Nagata,[†] Tsuyoshi Niahikawa,[†] and Michinori Suginome[*,†,‡]

[†]*Department of Synthetic Chemistry and Biological Chemistry, Graduate School of Engineering, Kyoto University, Katsura, Nishikyo-ku, Kyoto 615-8510 Japan, and* [‡]*CREST, Japan Science and Technology Agency (JST), Katsura, Nishikyo-ku, Kyoto 615-8510, Japan*

E-mail: suginome@sbchem.kyoto-u.ac.jp

Contents

[*]To whom correspondence should be addressed
[†]Department of Synthetic Chemistry and Biological Chemistry, Graduate School of Engineering, Kyoto University
[‡]JST, CREST

1 NMR Spectra of New Compounds

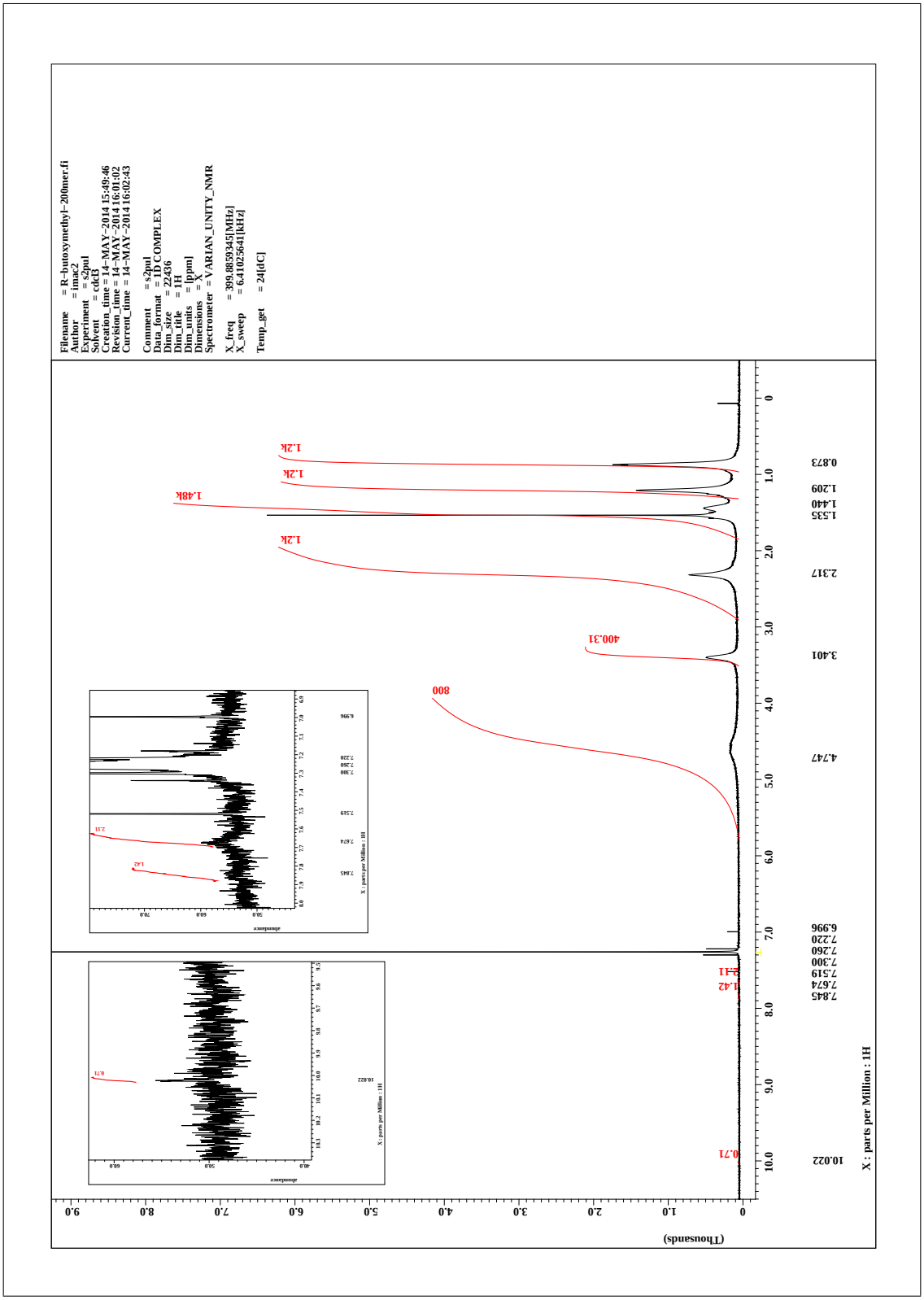

Figure S21. ^{1}H NMR spectrum of **1(200)** in $CDCl_3$.

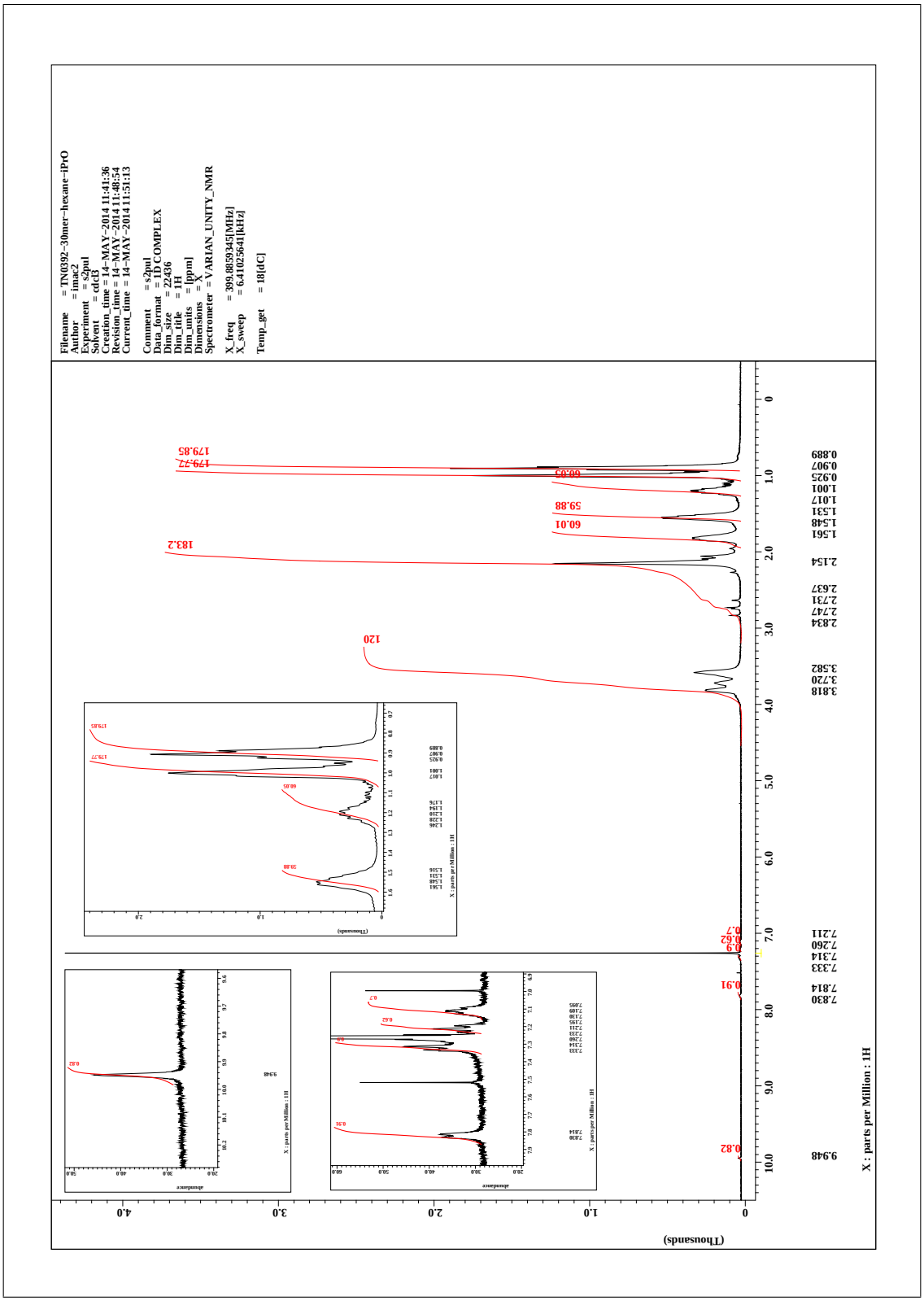

Figure S22. ^{1}H NMR spectrum of **3(30)** in $CDCl_3$.

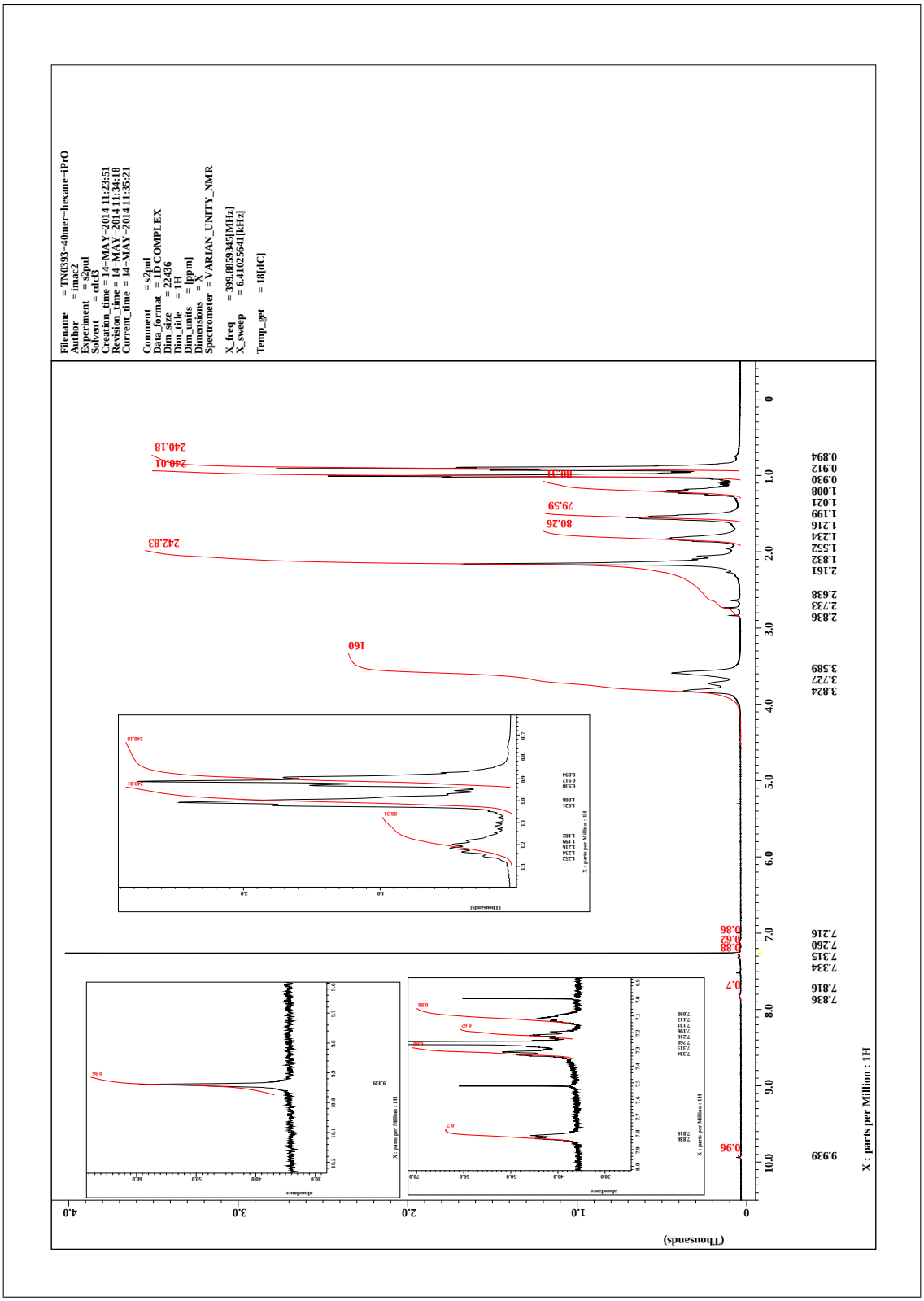

Figure S23. ^{1}H NMR spectrum of **3(40)** in $CDCl_3$.

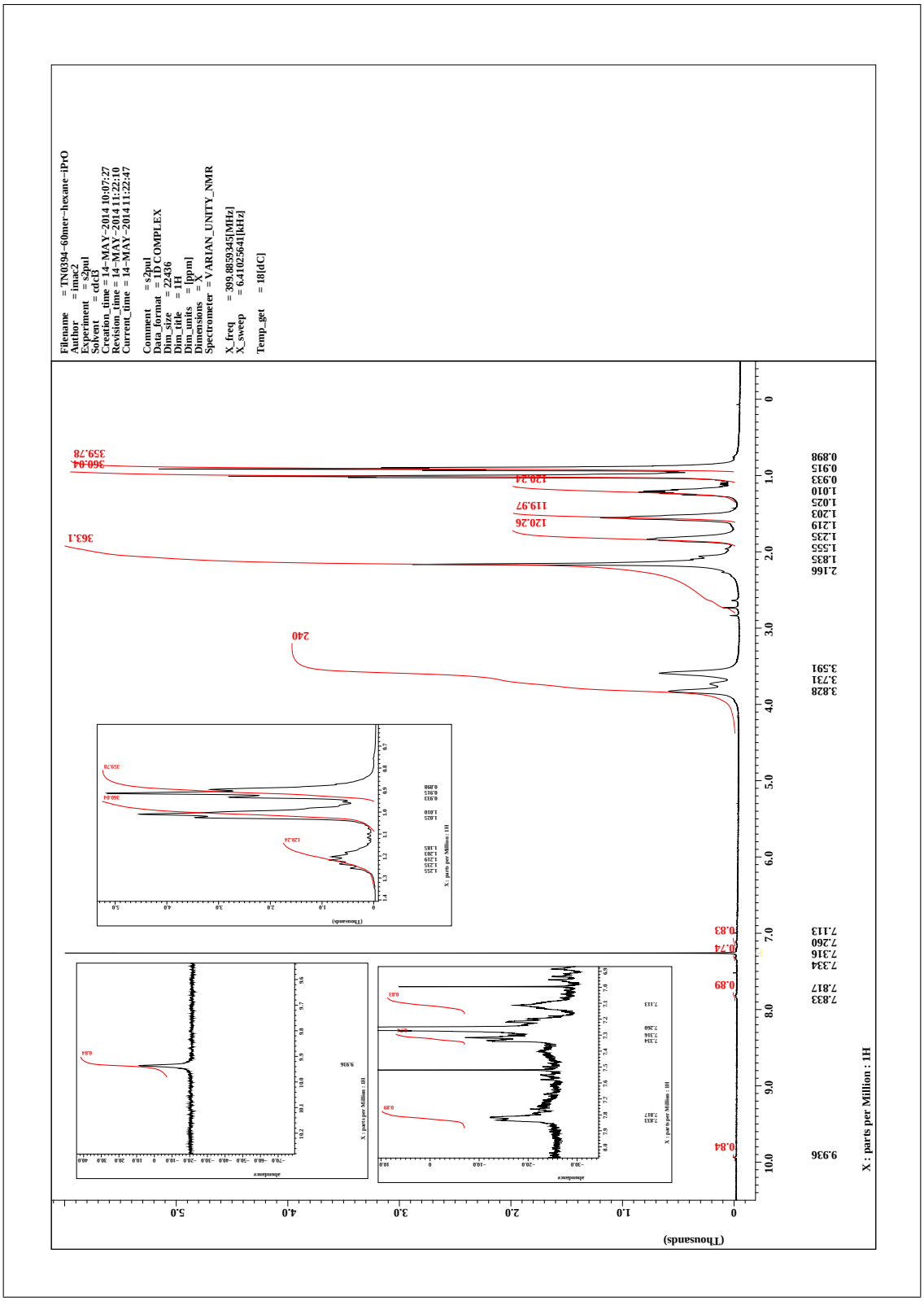

Figure S24. ^{1}H NMR spectrum of **3(60)** in $CDCl_3$.

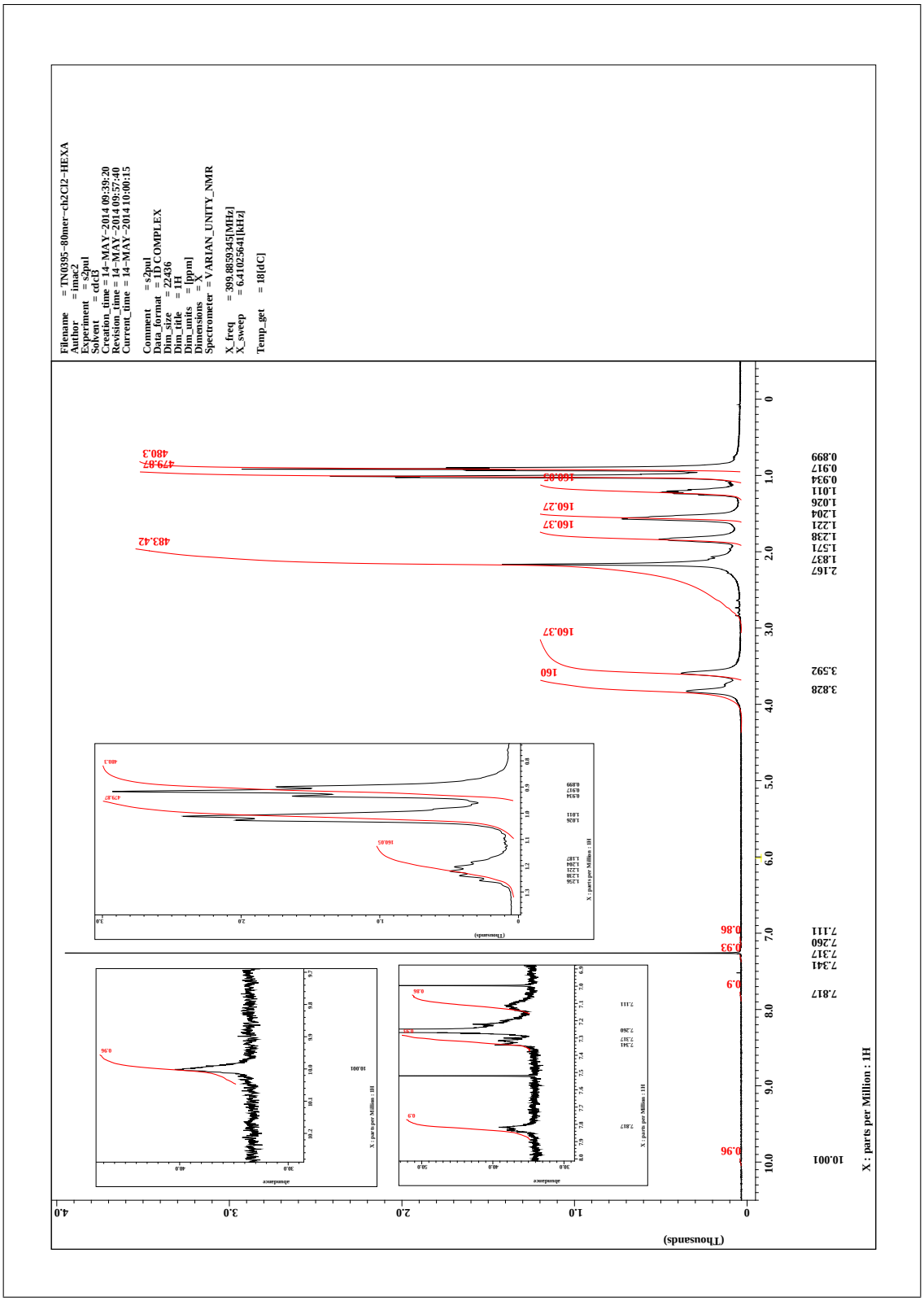

Figure S25. ^{1}H NMR spectrum of **3(80)** in $CDCl_3$.

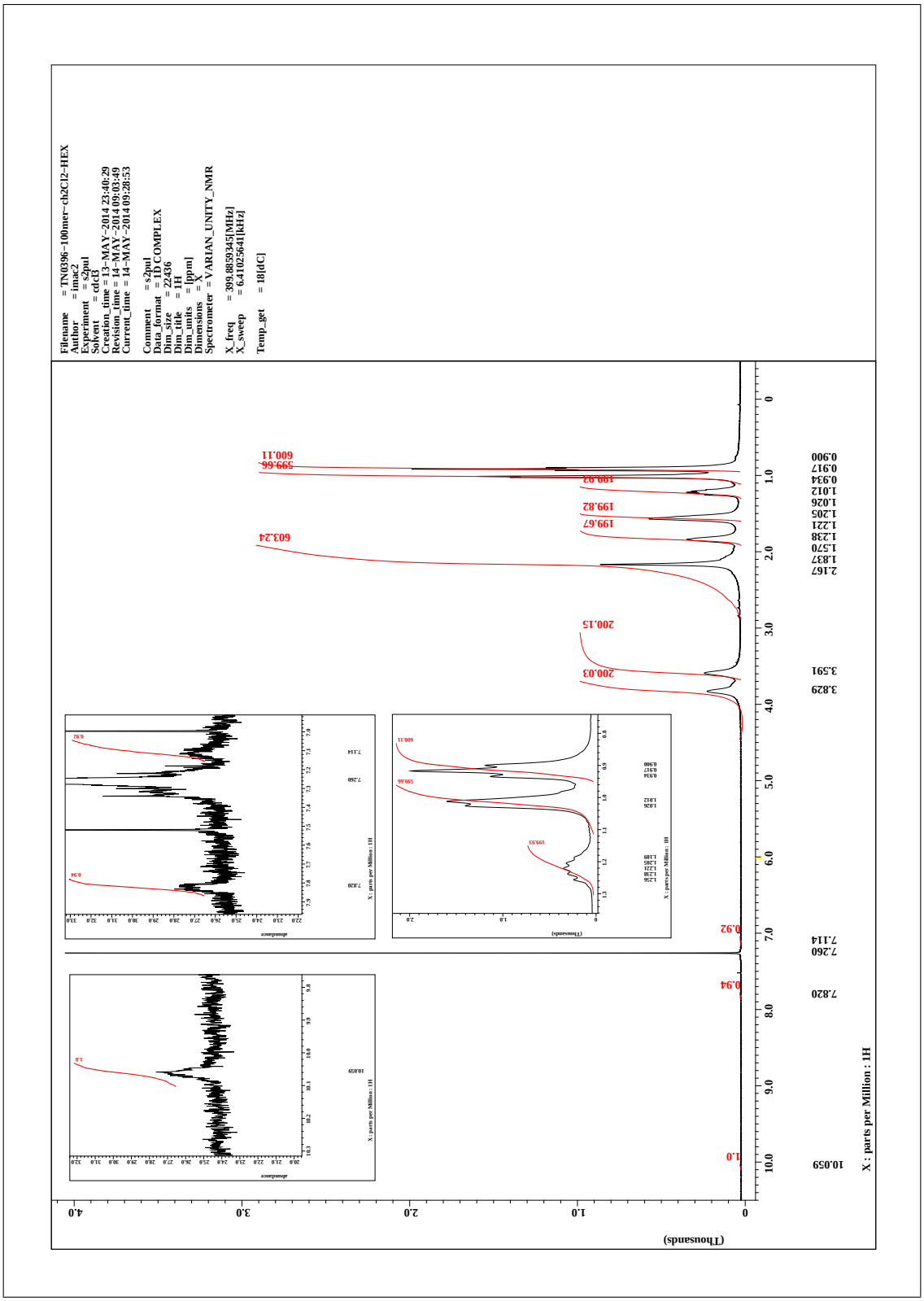

Figure S26. ^{1}H NMR spectrum of **3(100)** in $CDCl_3$.

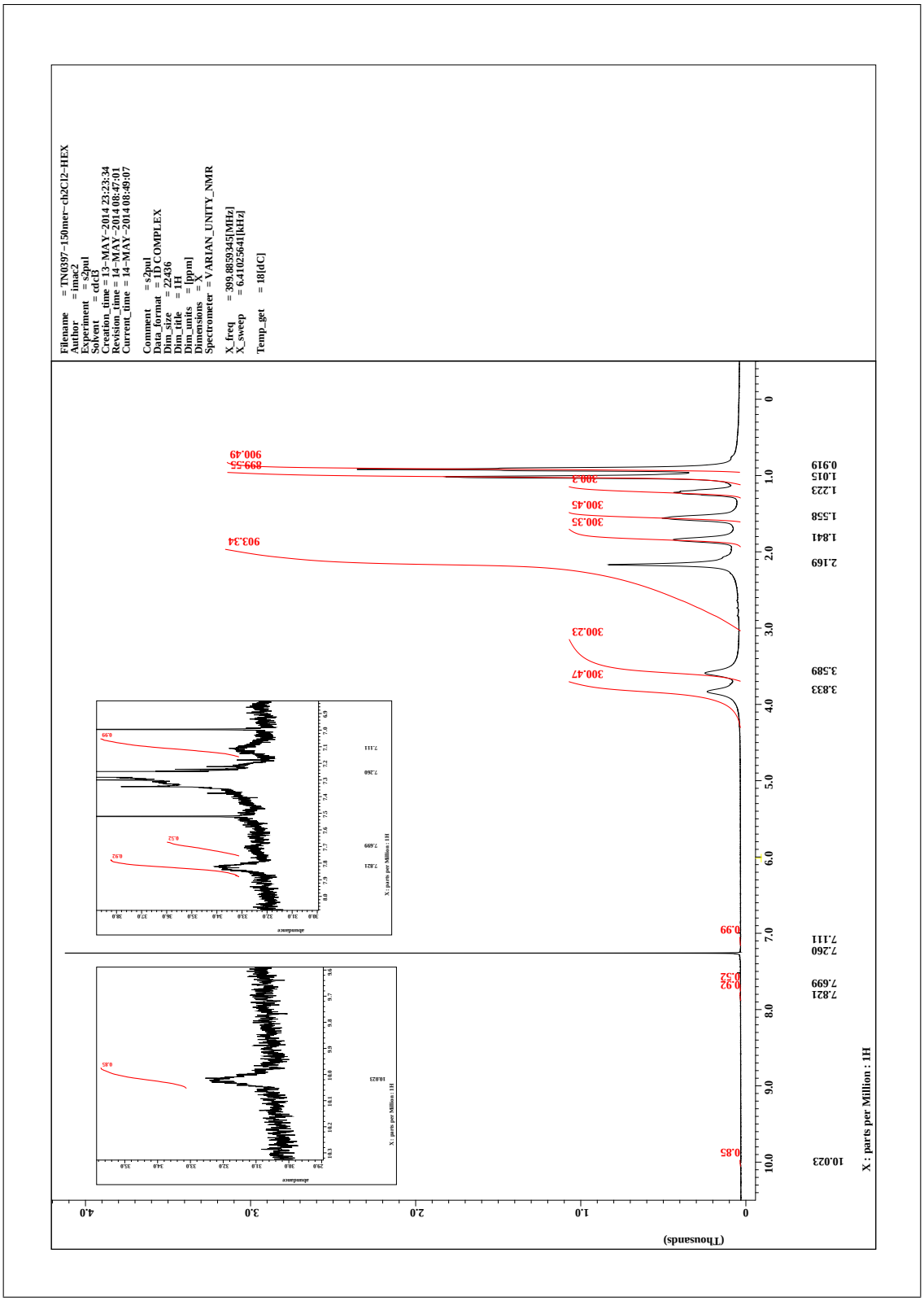

Figure S27. ^{1}H NMR spectrum of **3(150)** in $CDCl_3$.

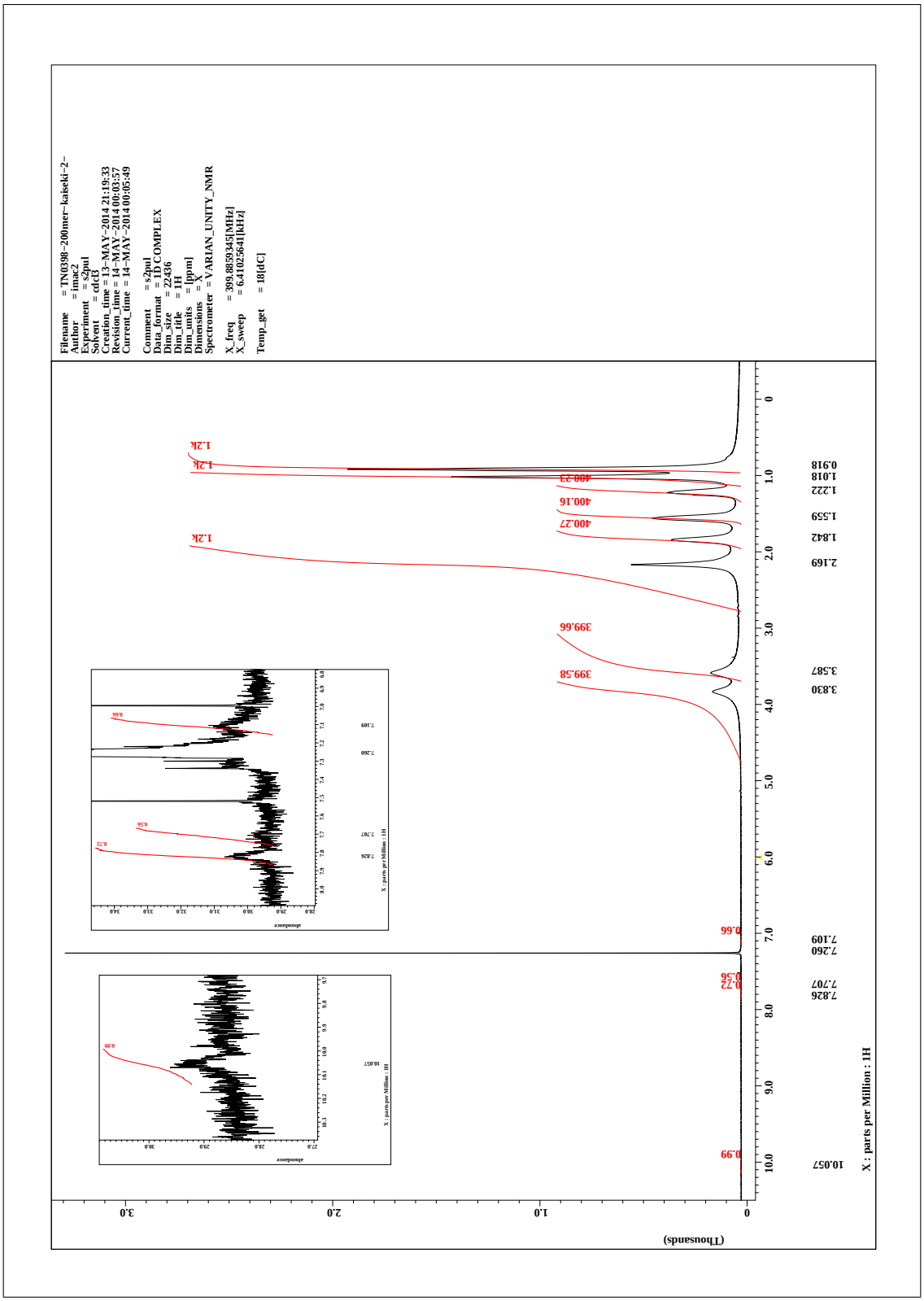

Figure S28. ^{1}H NMR spectrum of **3(200)** in $CDCl_3$.

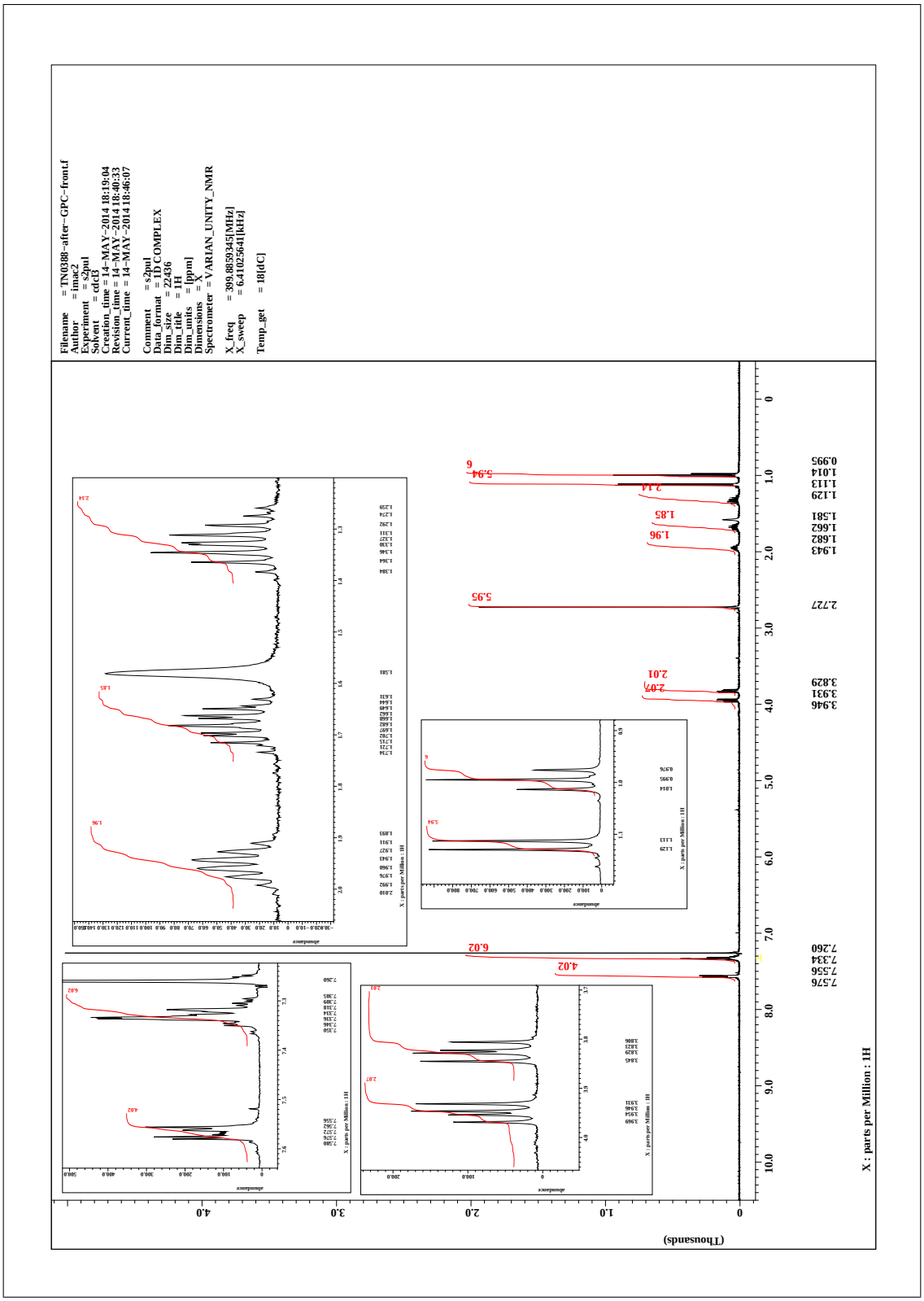

Figure S29. ^{1}H NMR spectrum of **4** in $CDCl_3$.

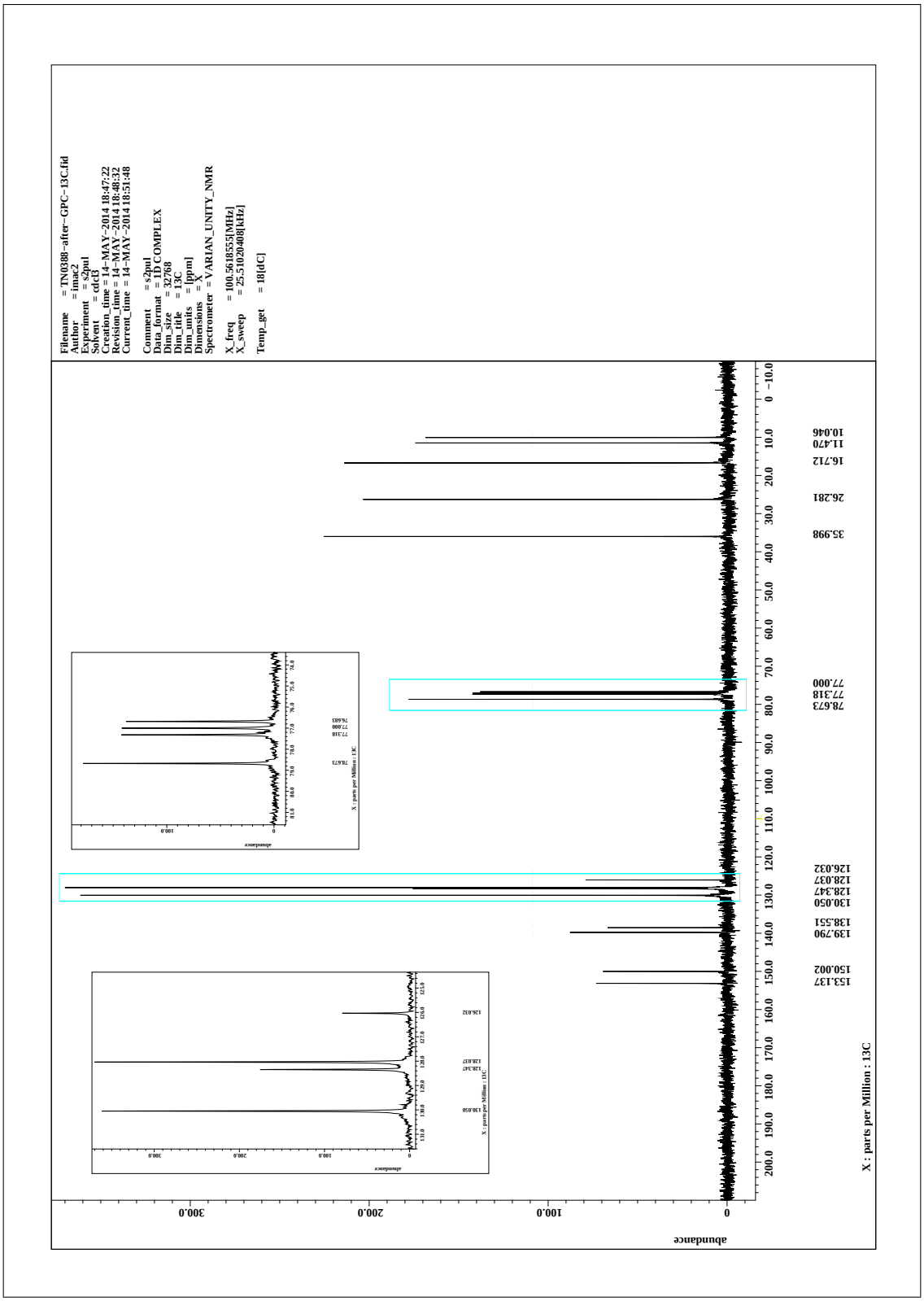

Figure S30. ^{13}C NMR spectrum of **4** in $CDCl_3$.

2 UV-vis and CD Spectra of New Compounds

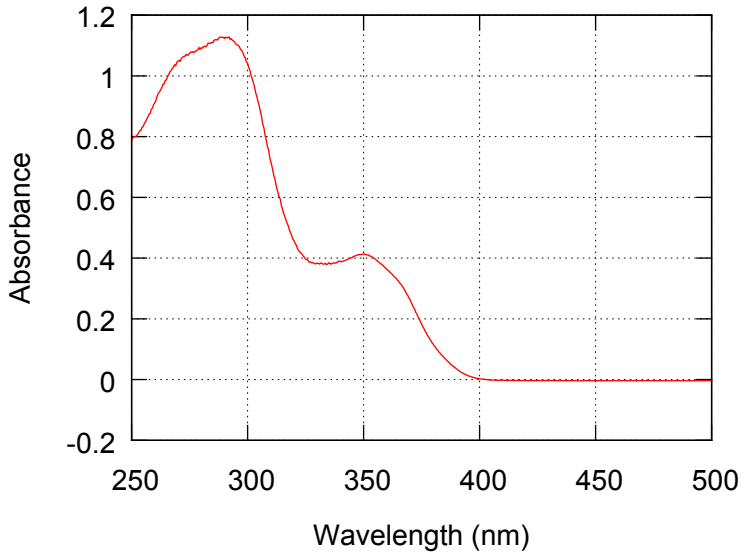

Figure S31. UV-vis absorption spectrum of **1(200)** in $CHCl_3$ (1.60×10^{-2} g/L, path length = 10 mm).

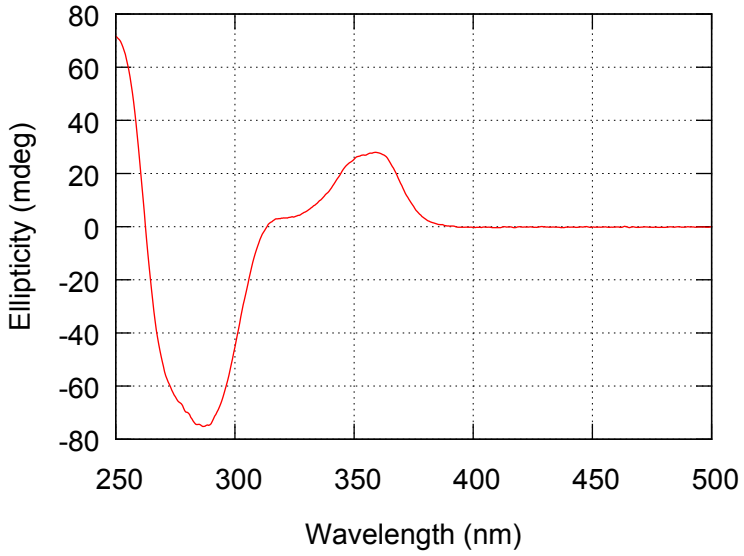

Figure S32. CD spectrum of **1(200)** in $CHCl_3$ (1.60×10^{-2} g/L, path length = 10 mm).

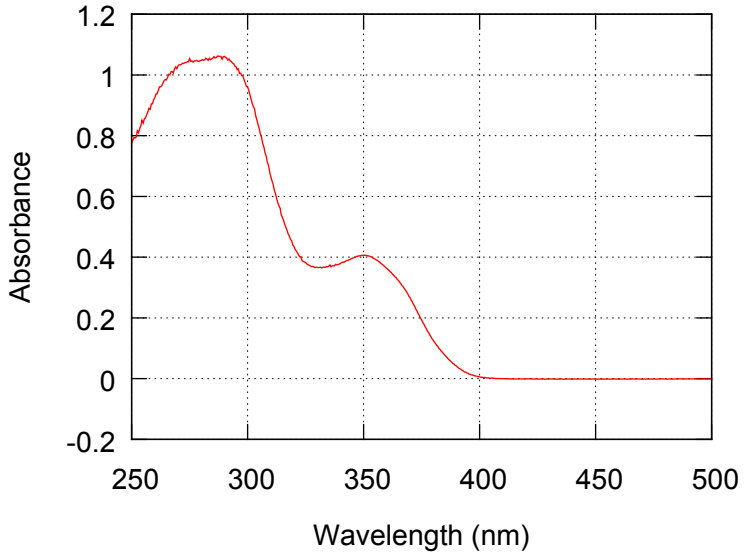

Figure S33. UV-vis absorption spectrum of **1(200)** in 1,1,1-TCE (1.60×10^{-2} g/L, path length = 10 mm).

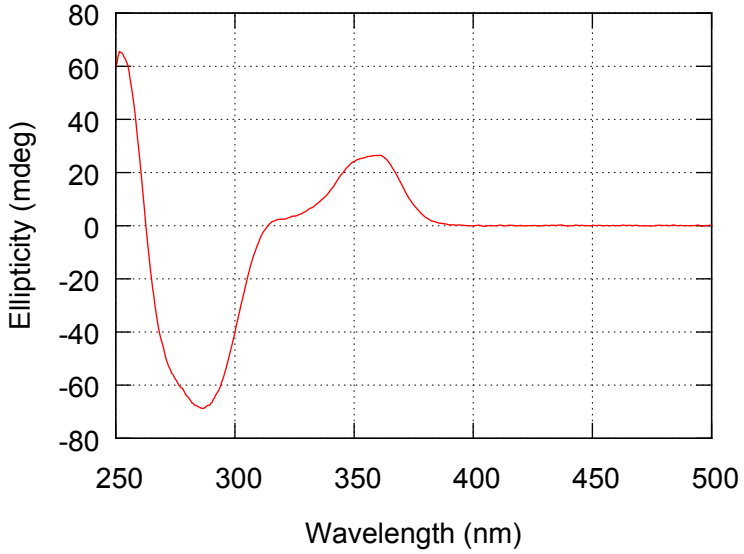

Figure S34. CD spectrum of **1(200)** in 1,1,1-TCE (1.60×10^{-2} g/L, path length = 10 mm).

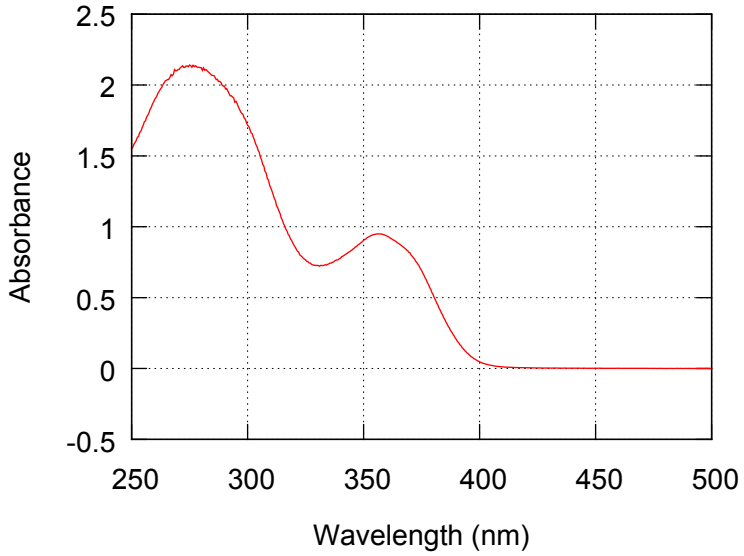

Figure S35. UV-vis absorption spectrum of **2(200)** in $CHCl_3$ (2.36×10^{-2} g/L, path length = 10 mm).

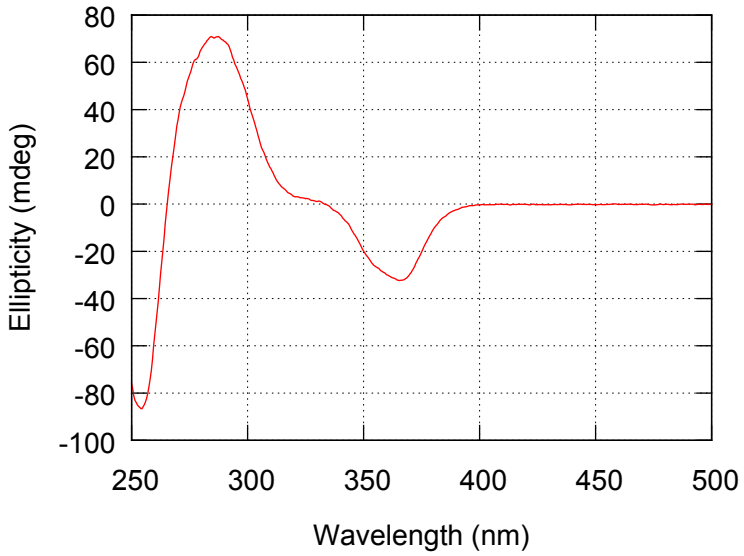

Figure S36. CD spectrum of **2(200)** in $CHCl_3$ (2.36×10^{-2} g/L, path length = 10 mm).

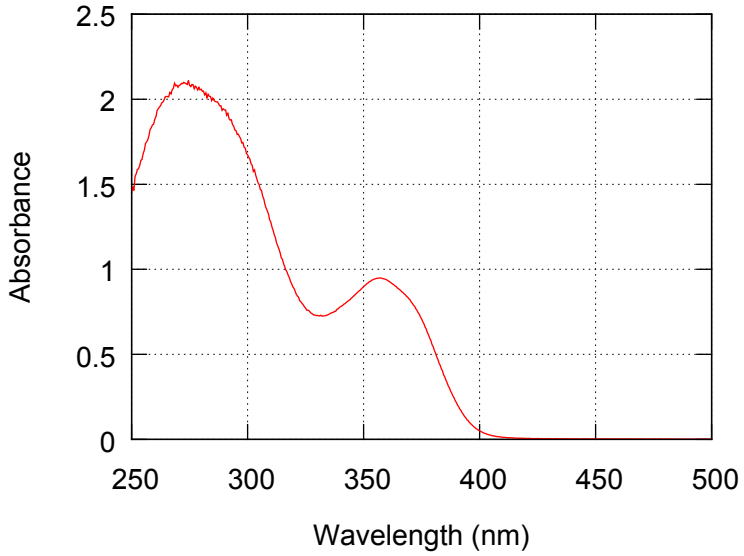

Figure S37. UV-vis absorption spectrum of **2(200)** in 1,1,1-TCE (2.36×10^{-2} g/L, path length = 10 mm).

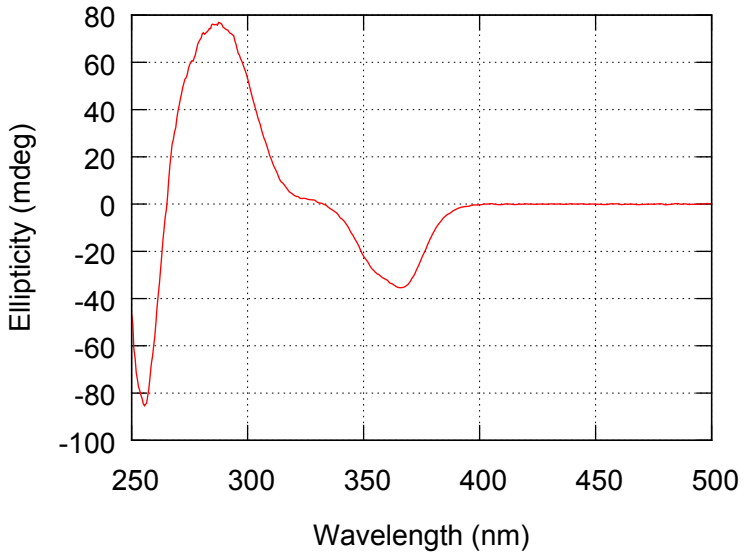

Figure S38. CD spectrum of **2(200)** in 1,1,1-TCE (2.36×10^{-2} g/L, path length = 10 mm).

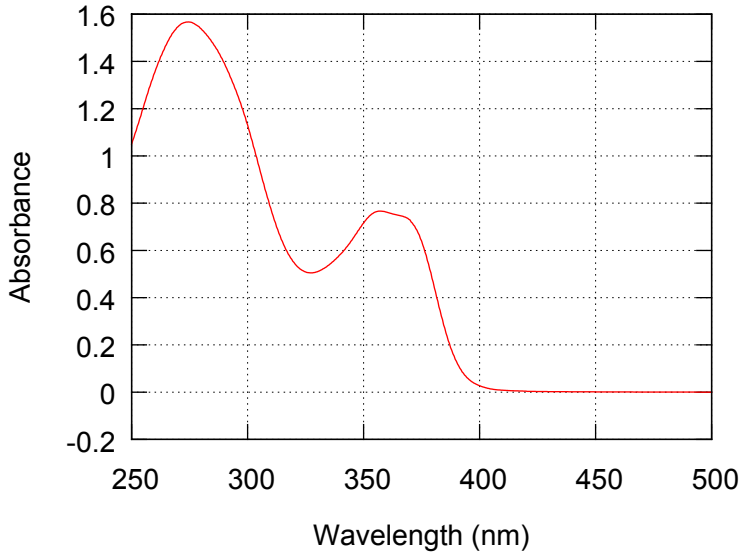

Figure S39. UV-vis absorption spectrum of **3(30)** in $CHCl_3$ (2.08×10^{-2} g/L, path length = 10 mm).

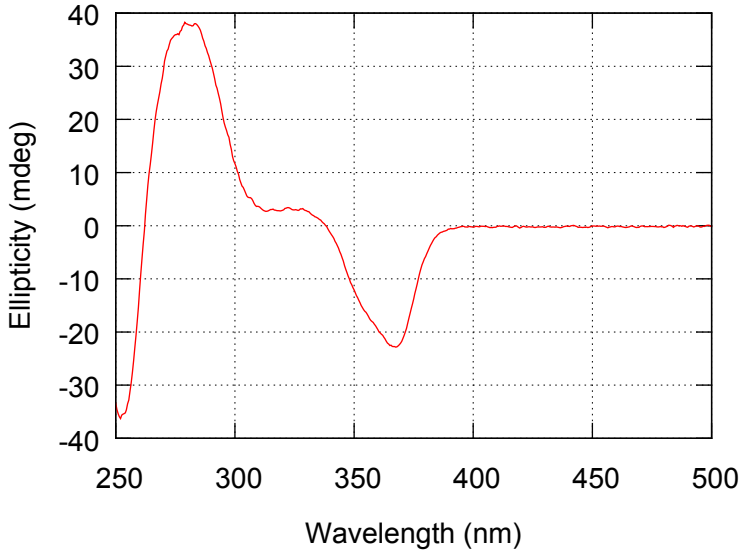

Figure S40. CD spectrum of **3(30)** in $CHCl_3$ (2.08×10^{-2} g/L, path length = 10 mm).

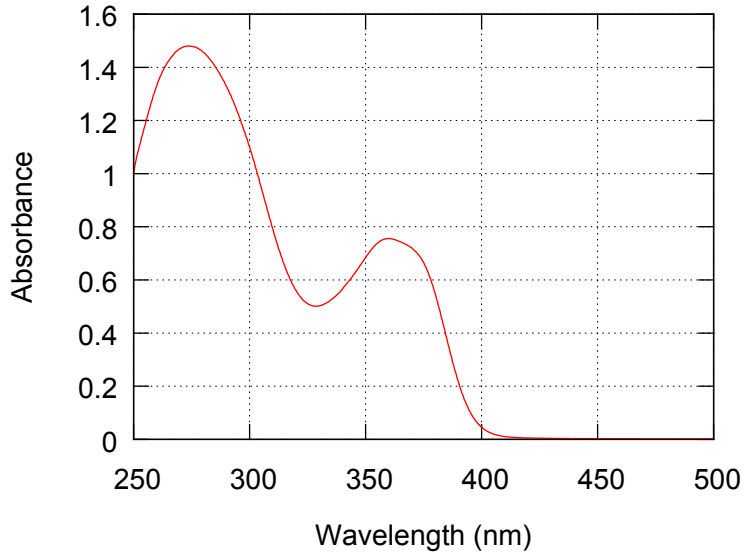

Figure S41. UV-vis absorption spectrum of **3(30)** in 1,1,1-TCE (2.08×10^{-2} g/L, path length = 10 mm).

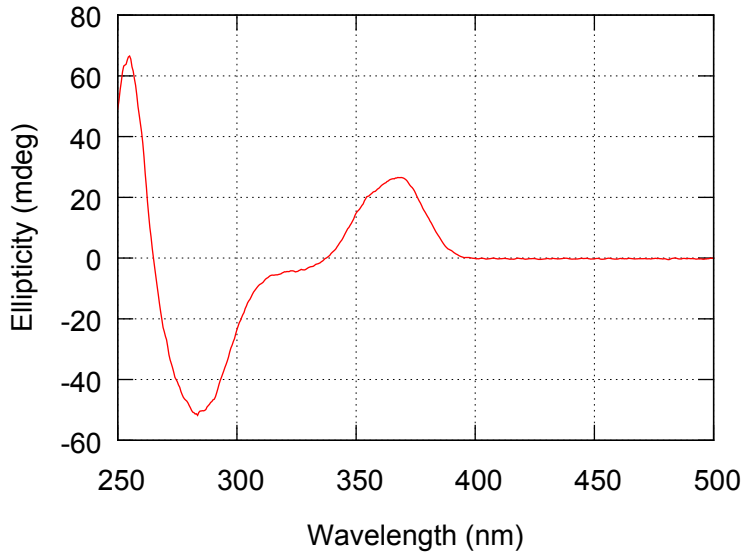

Figure S42. CD spectrum of **3(30)** in 1,1,1-TCE (2.08×10^{-2} g/L, path length = 10 mm).

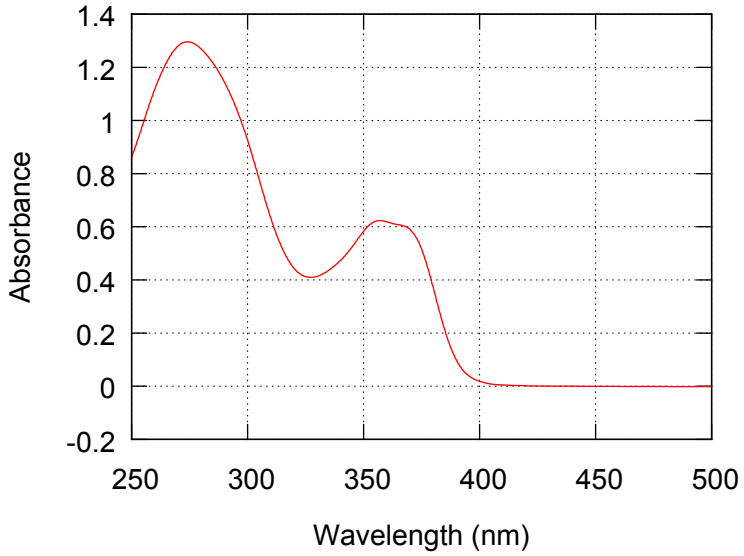

Figure S43. UV-vis absorption spectrum of **3(40)** in $CHCl_3$ (2.09×10^{-2} g/L, path length = 10 mm).

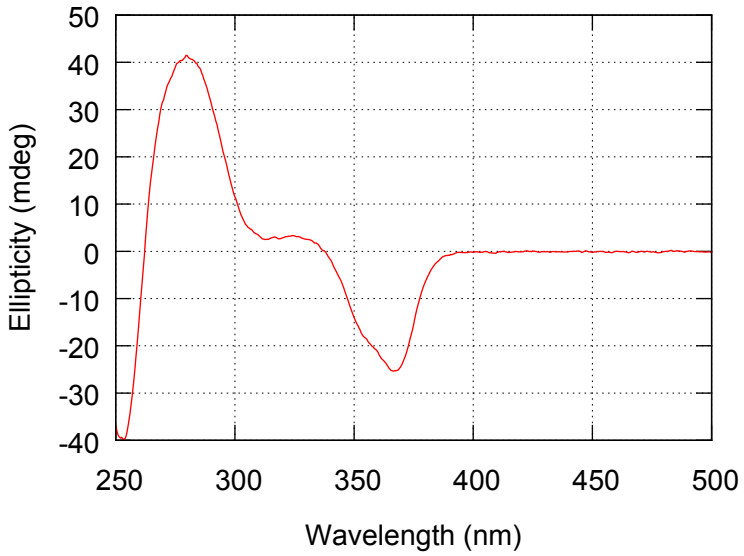

Figure S44. CD spectrum of **3(40)** in $CHCl_3$ (2.09×10^{-2} g/L, path length = 10 mm).

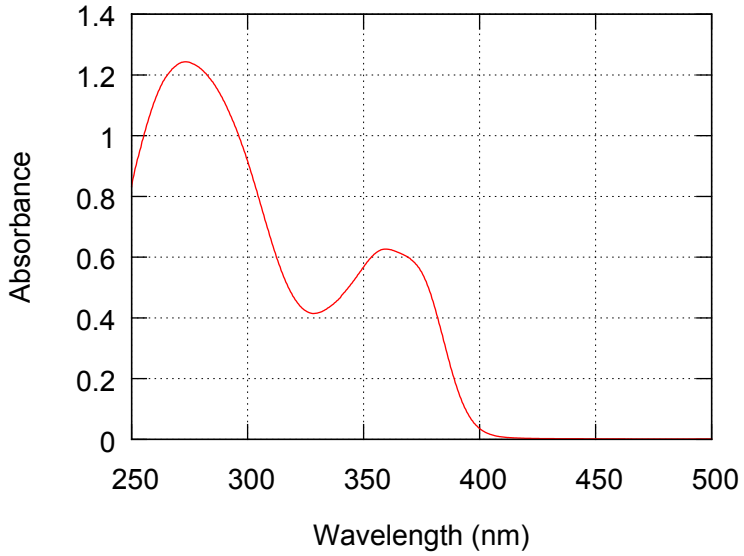

Figure S45. UV-vis absorption spectrum of **3(40)** in 1,1,1-TCE (2.09×10^{-2} g/L, path length = 10 mm).

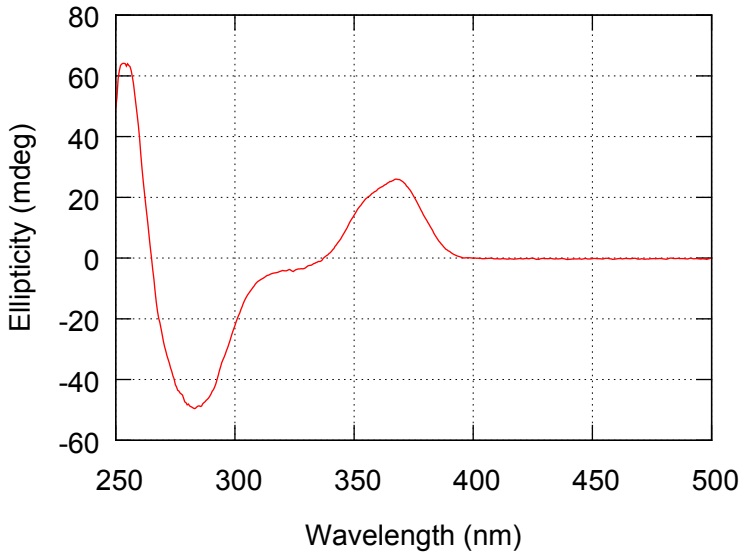

Figure S46. CD spectrum of **3(40)** in 1,1,1-TCE (2.09×10^{-2} g/L, path length = 10 mm).

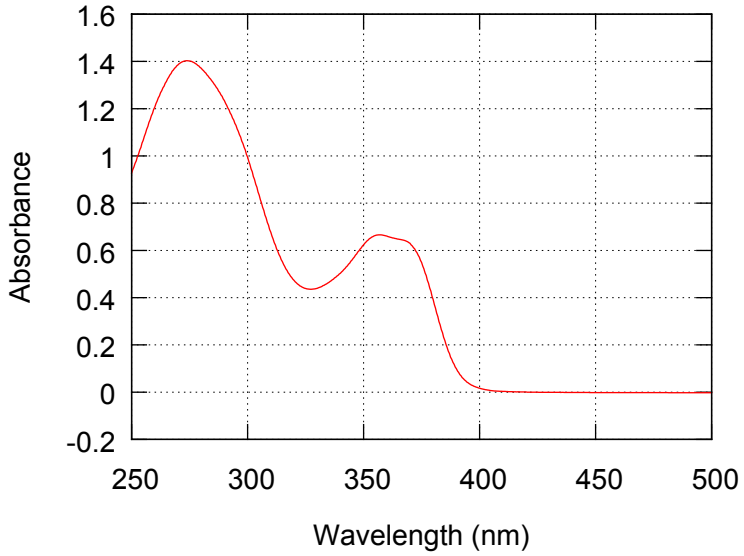

Figure S47. UV-vis absorption spectrum of **3(60)** in $CHCl_3$ (2.70×10^{-2} g/L, path length = 10 mm).

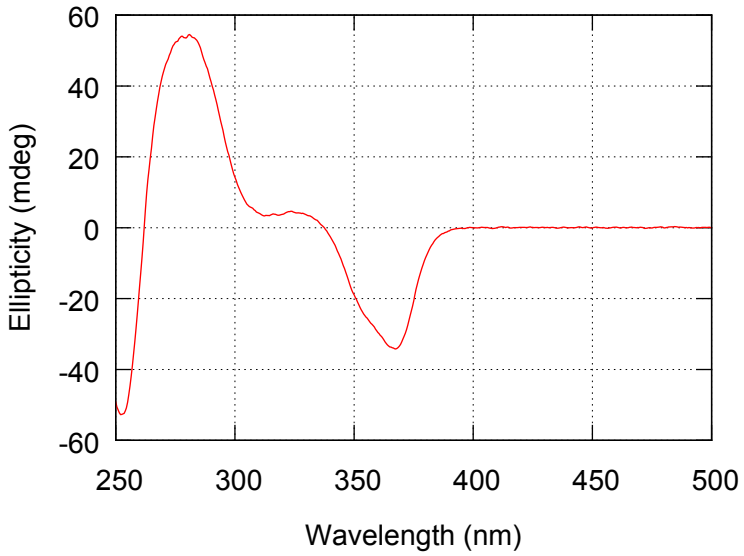

Figure S48. CD spectrum of **3(60)** in $CHCl_3$ (2.70×10^{-2} g/L, path length = 10 mm).

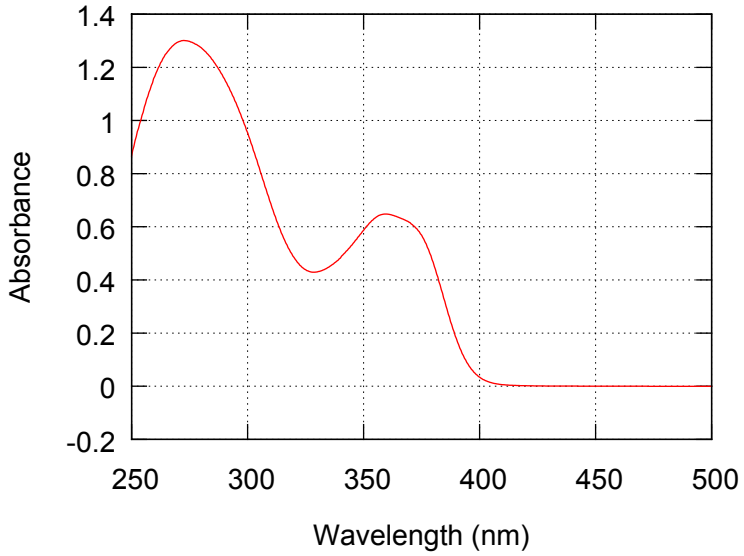

Figure S49. UV-vis absorption spectrum of **3(60)** in 1,1,1-TCE (2.70×10^{-2} g/L, path length = 10 mm).

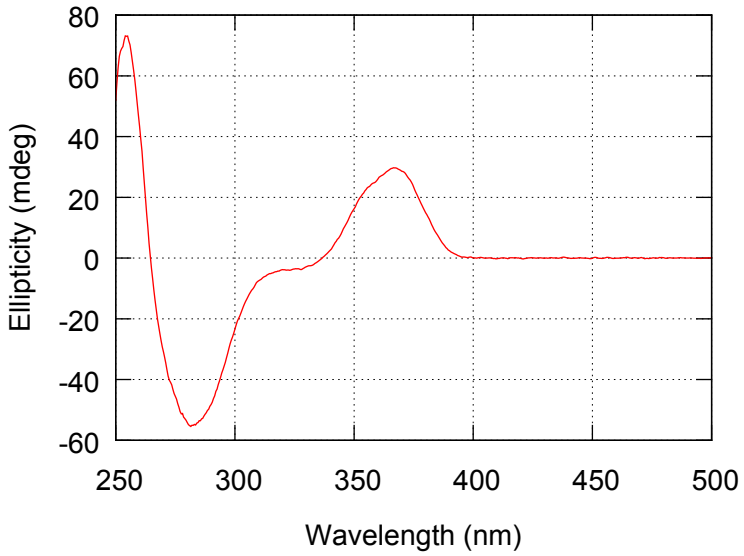

Figure S50. CD spectrum of **3(60)** in 1,1,1-TCE (2.70×10^{-2} g/L, path length = 10 mm).

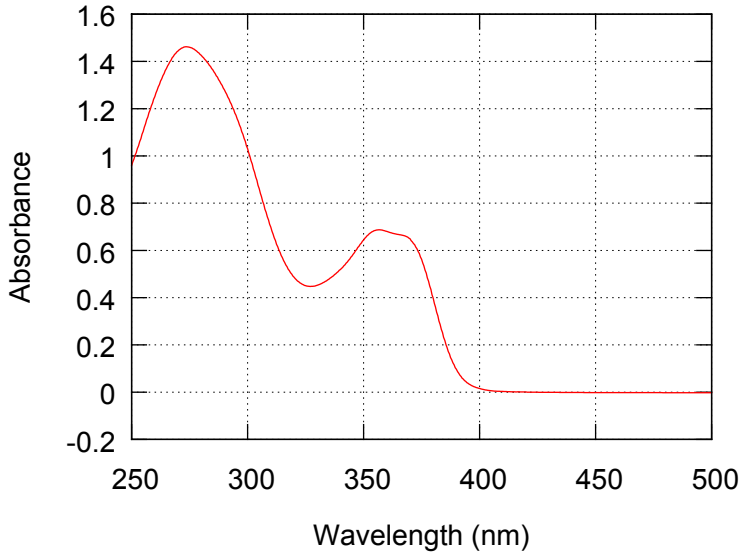

Figure S51. UV-vis absorption spectrum of **3(80)** in $CHCl_3$ (2.90×10^{-2} g/L, path length = 10 mm).

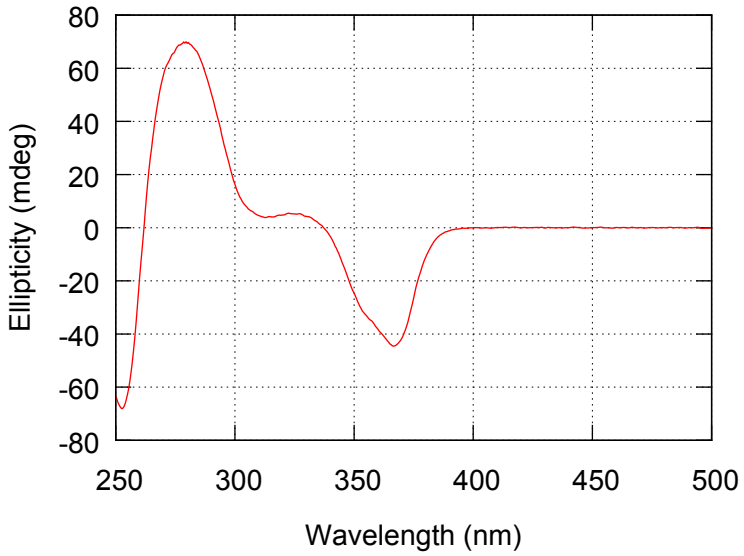

Figure S52. CD spectrum of **3(80)** in $CHCl_3$ (2.90×10^{-2} g/L, path length = 10 mm).

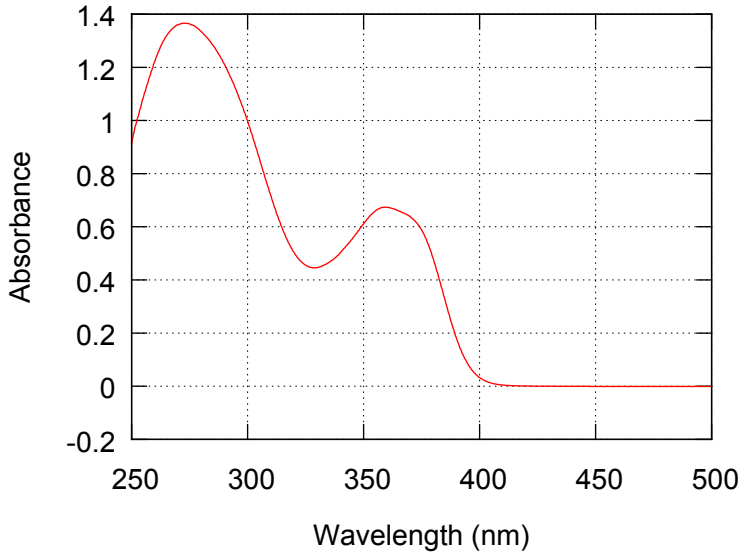

Figure S53. UV-vis absorption spectrum of **3(80)** in 1,1,1-TCE (2.90×10^{-2} g/L, path length = 10 mm).

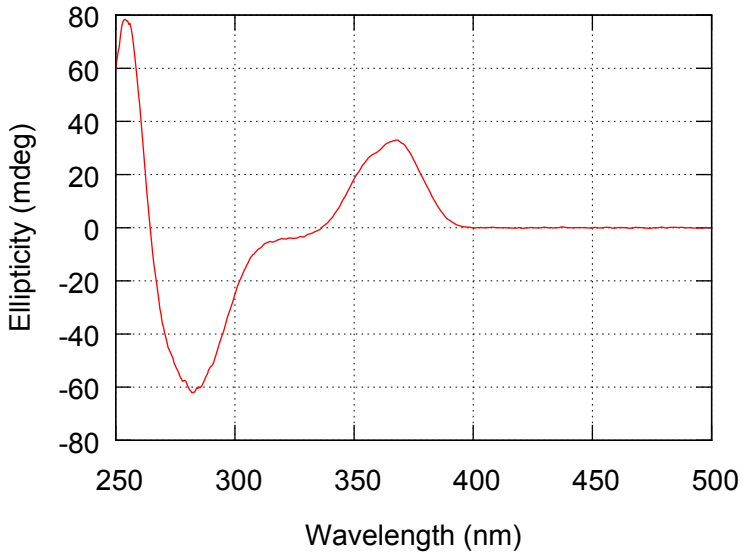

Figure S54. CD spectrum of **3(80)** in 1,1,1-TCE (2.90×10^{-2} g/L, path length = 10 mm).

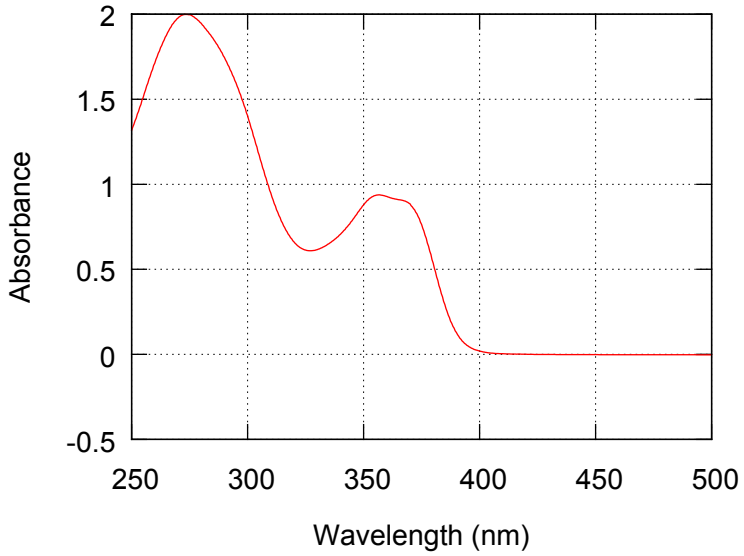

Figure S55. UV-vis absorption spectrum of **3(100)** in $CHCl_3$ (3.29×10^{-2} g/L, path length = 10 mm).

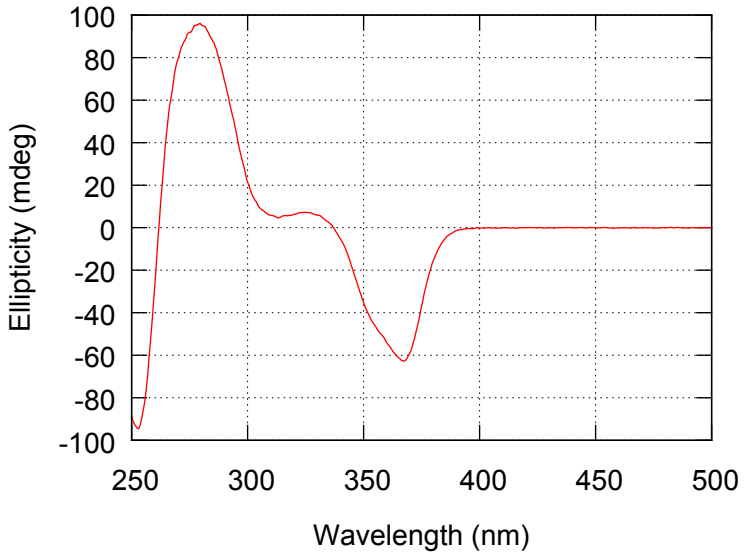

Figure S56. CD spectrum of **3(100)** in $CHCl_3$ (3.29×10^{-2} g/L, path length = 10 mm).

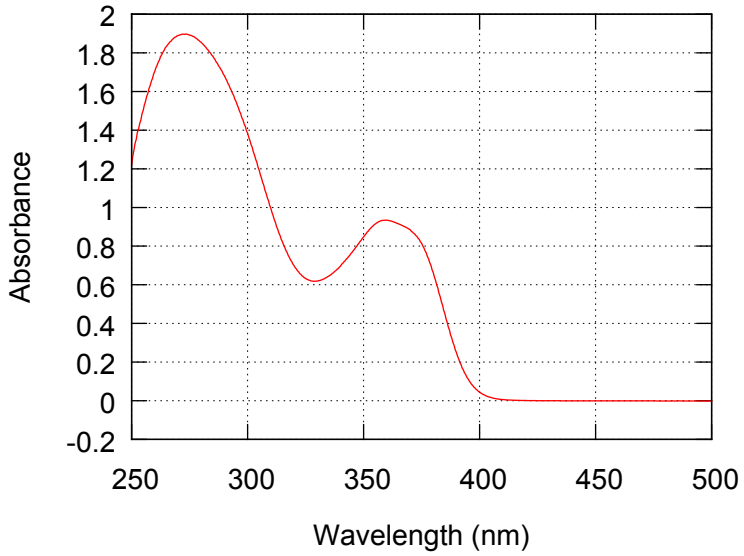

Figure S57. UV-vis absorption spectrum of **3(100)** in 1,1,1-TCE (3.29×10^{-2} g/L, path length = 10 mm).

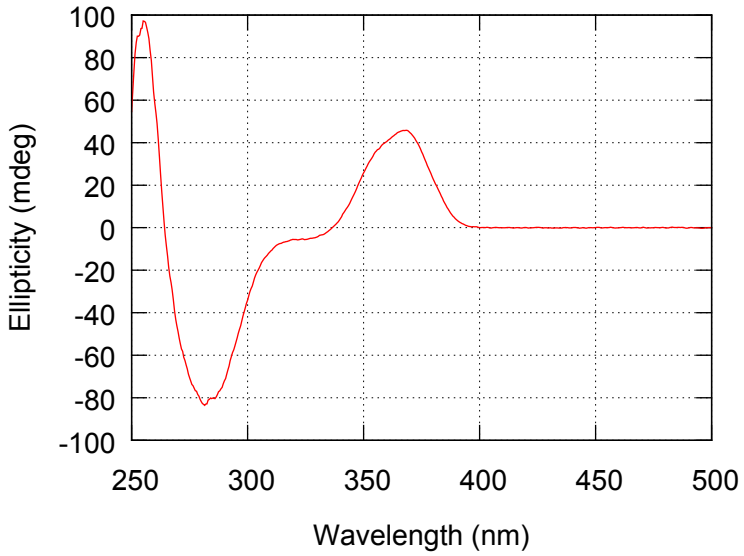

Figure S58. CD spectrum of **3(100)** in 1,1,1-TCE (3.29×10^{-2} g/L, path length = 10 mm).

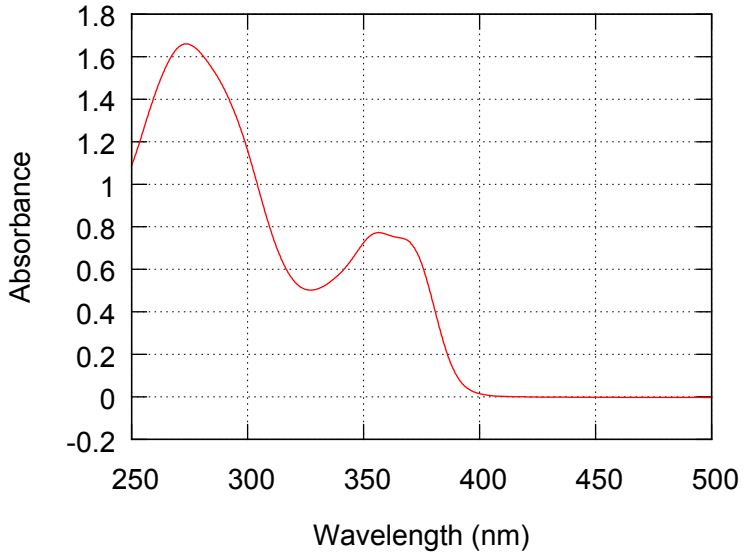

Figure S59. UV-vis absorption spectrum of **3(150)** in $CHCl_3$ (2.83×10^{-2} g/L, path length = 10 mm).

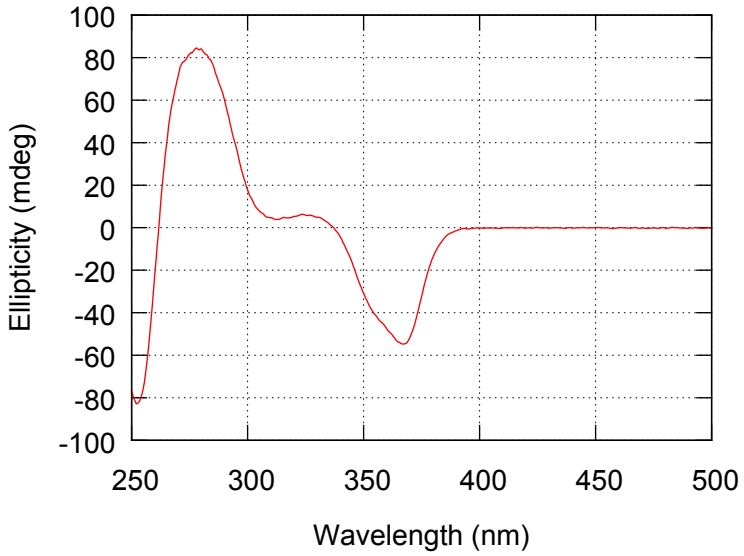

Figure S60. CD spectrum of **3(150)** in $CHCl_3$ (2.83×10^{-2} g/L, path length = 10 mm).

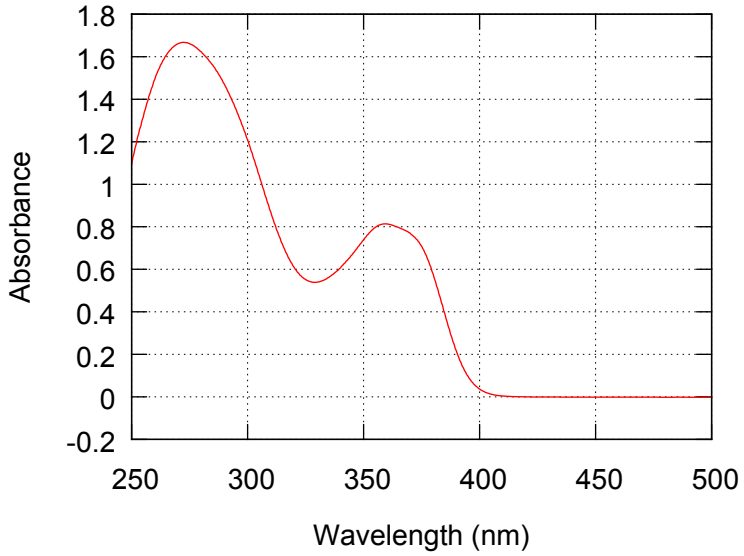

Figure S61. UV-vis absorption spectrum of **3(150)** in 1,1,1-TCE (2.83×10^{-2} g/L, path length = 10 mm).

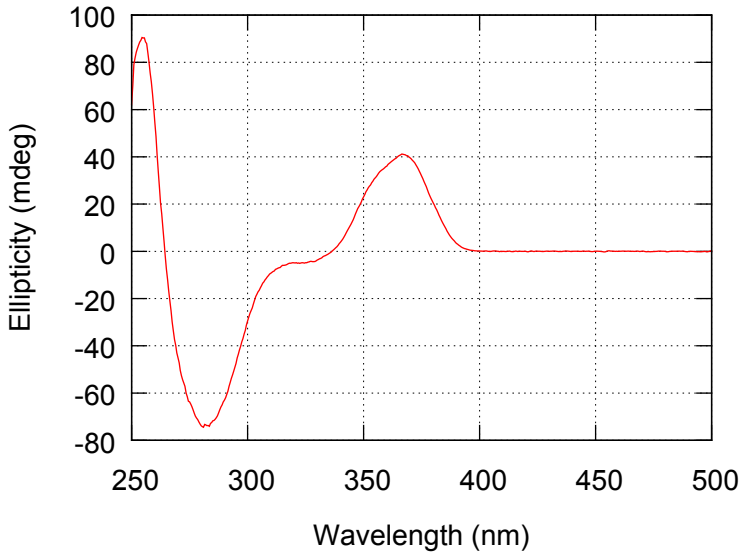

Figure S62. CD spectrum of **3(150)** in 1,1,1-TCE (2.83×10^{-2} g/L, path length = 10 mm).

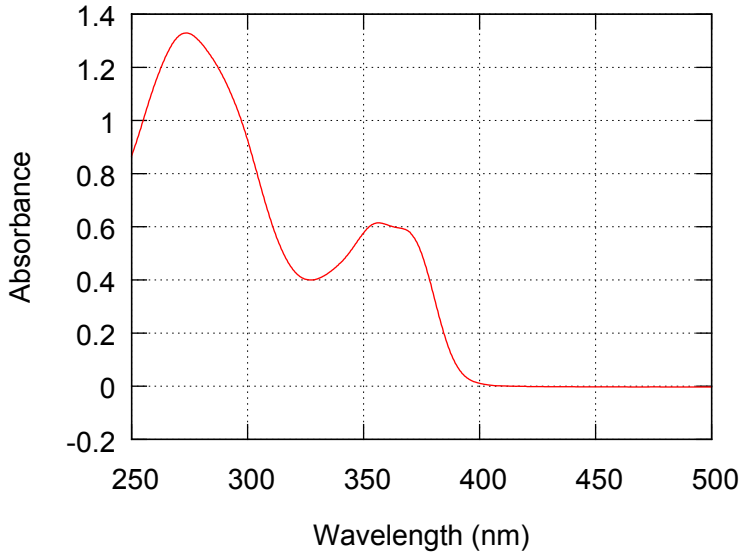

Figure S63. UV-vis absorption spectrum of **3(200)** in $CHCl_3$ (2.12×10^{-2} g/L, path length = 10 mm).

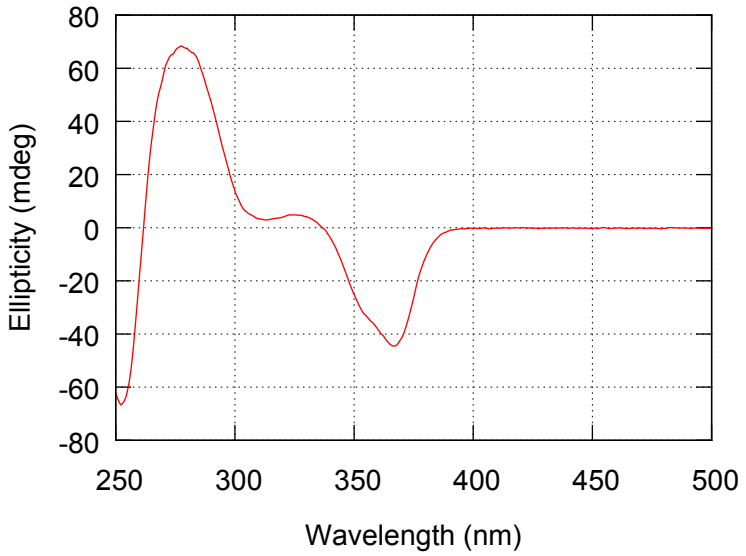

Figure S64. CD spectrum of **3(200)** in $CHCl_3$ (2.12×10^{-2} g/L, path length = 10 mm).

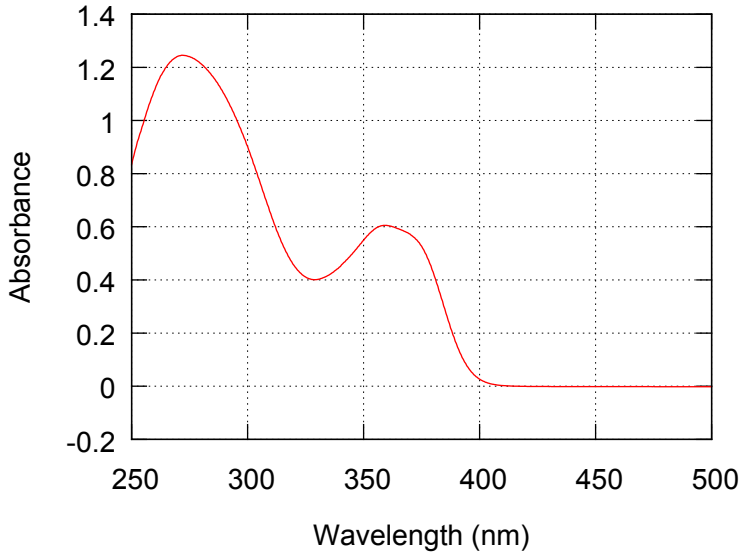

Figure S65. UV-vis absorption spectrum of **3(200)** in 1,1,1-TCE (2.12×10^{-2} g/L, path length = 10 mm).

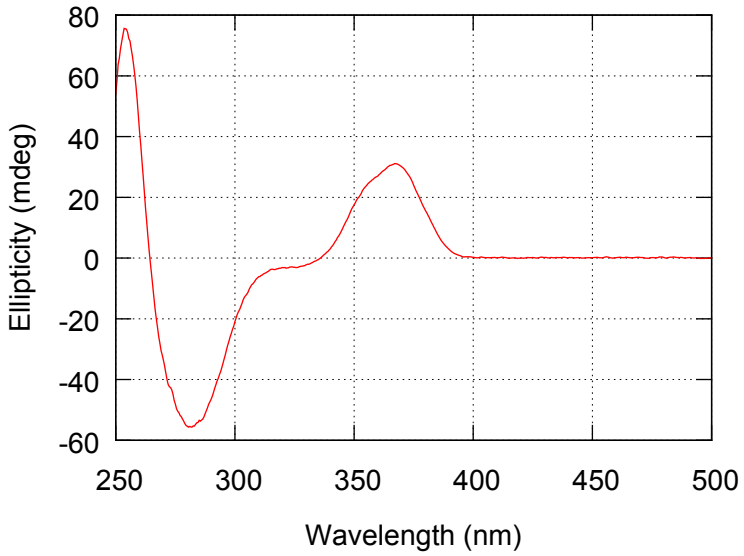

Figure S66. CD spectrum of **3(200)** in 1,1,1-TCE (2.12×10^{-2} g/L, path length = 10 mm).

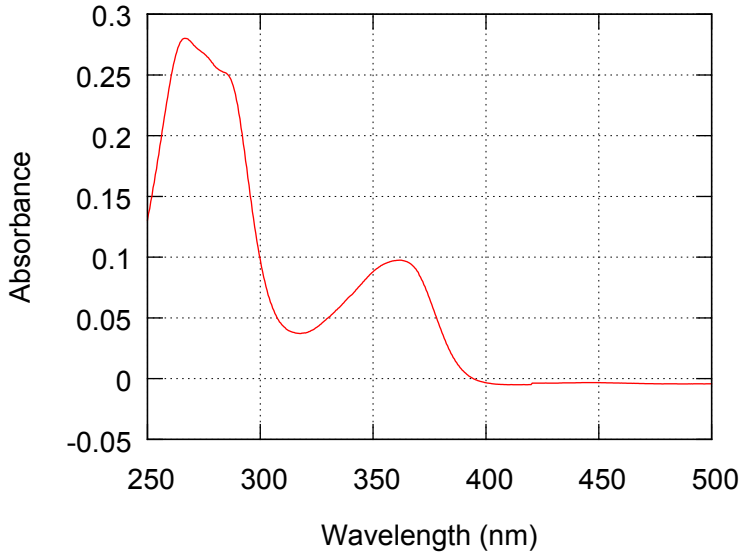

Figure S67. UV-vis absorption spectrum of **4** in $CHCl_3$ (4.82×10^{-3} g/L, path length = 10 mm).

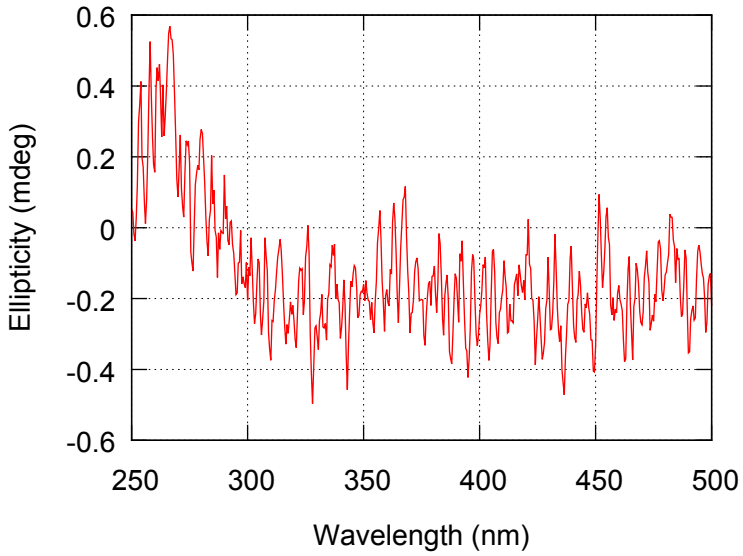

Figure S68. CD spectrum of **4** in $CHCl_3$ (4.82×10^{-3} g/L, path length = 10 mm).

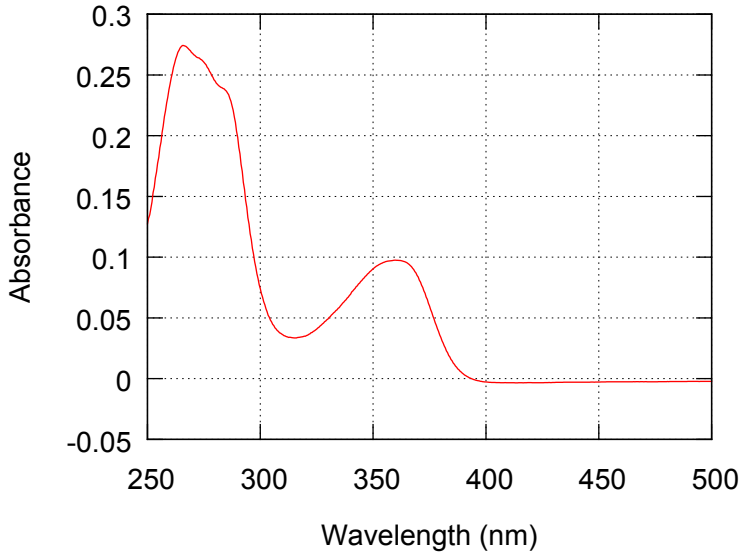

Figure S69. UV-vis absorption spectrum of **4** in 1,1,1-TCE (4.82×10^{-3} g/L, path length = 10 mm).

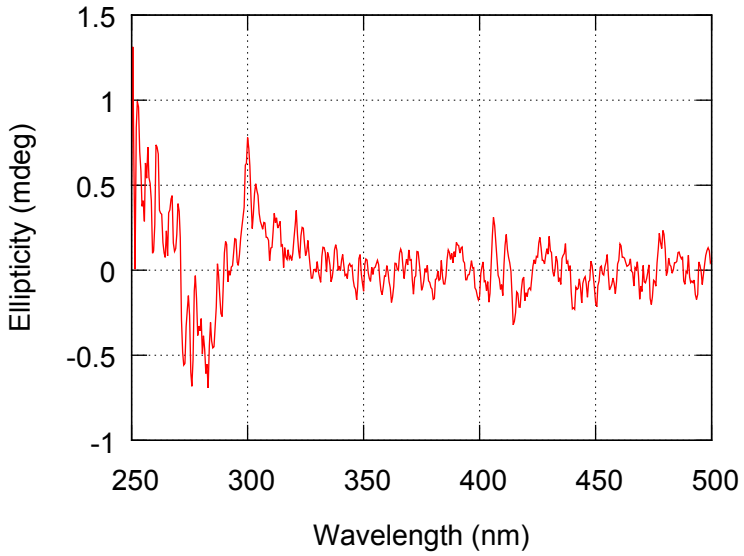

Figure S70. CD spectrum of **4** in 1,1,1-TCE (4.82×10^{-3} g/L, path length = 10 mm).

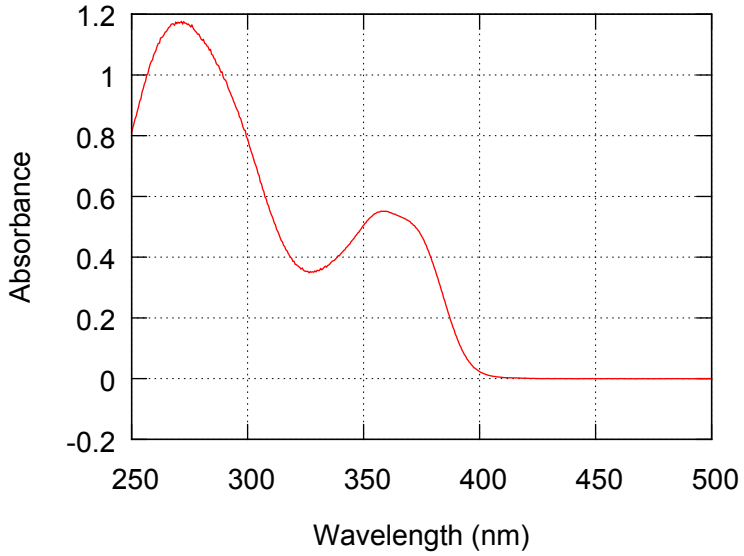

Figure S71. UV-vis absorption spectrum of **3(200)** in 1-BuCl (2.22×10^{-2} g/L, path length = 10 mm).

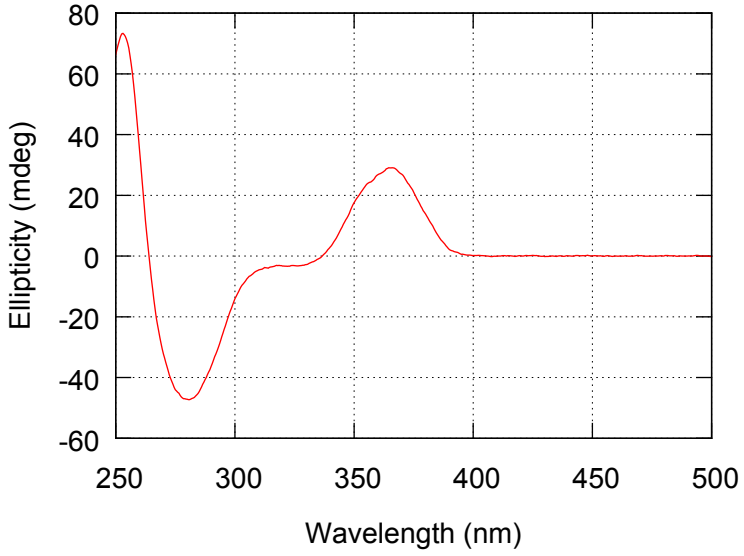

Figure S72. CD spectrum of **3(200)** in 1-BuCl (2.22×10^{-2} g/L, path length = 10 mm).

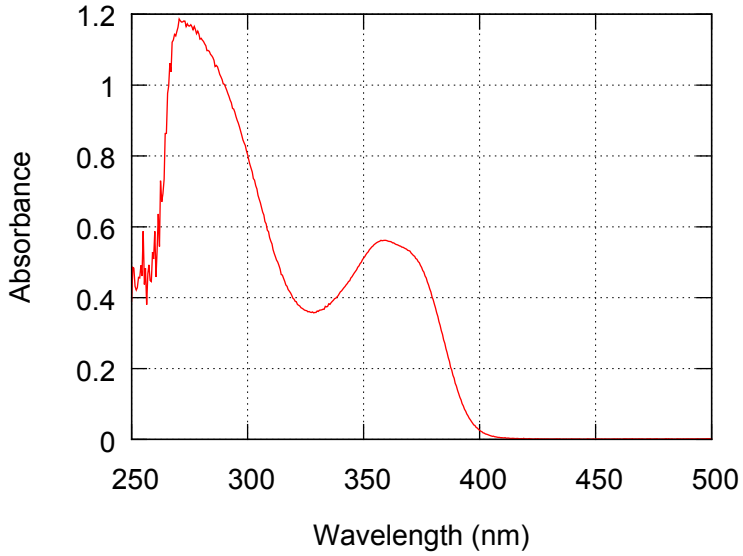

Figure S73. UV-vis absorption spectrum of **3(200)** in 1- BuBr (2.22×10^{-2} g/L, path length = 10 mm).

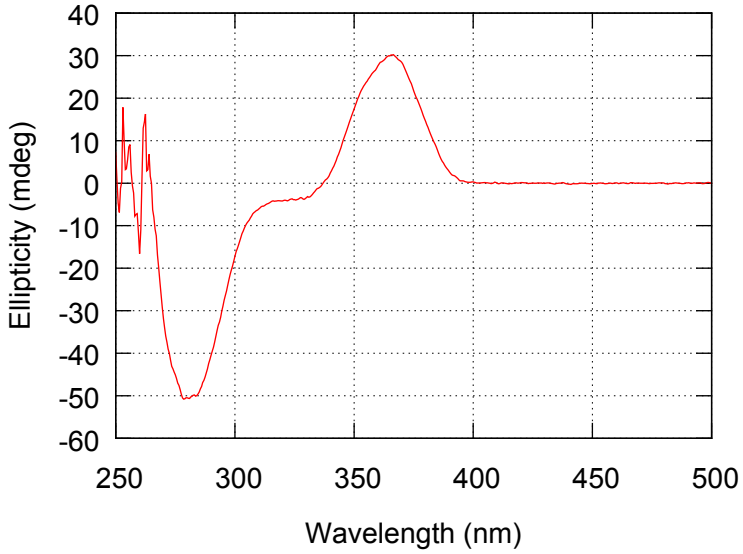

Figure S74. CD spectrum of **3(200)** in 1- BuBr (2.22×10^{-2} g/L, path length = 10 mm).

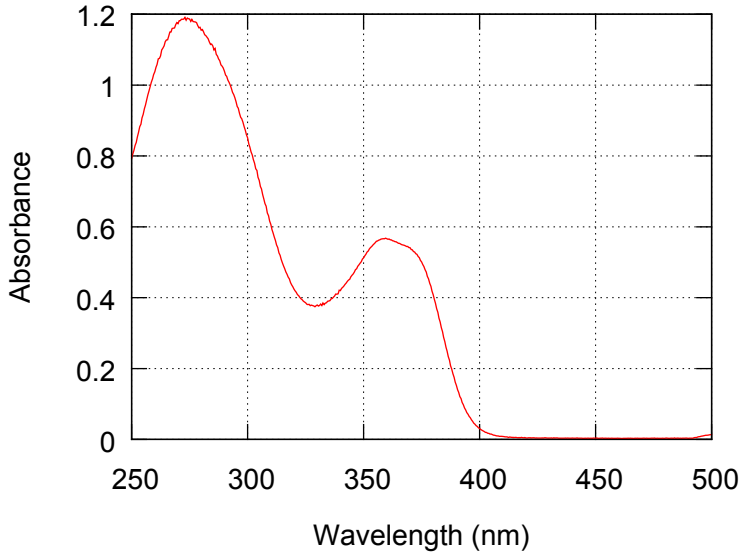

Figure S75. UV-vis absorption spectrum of **3(200)** in CH_2Cl_2 (2.22×10^{-2} g/L, path length = 10 mm).

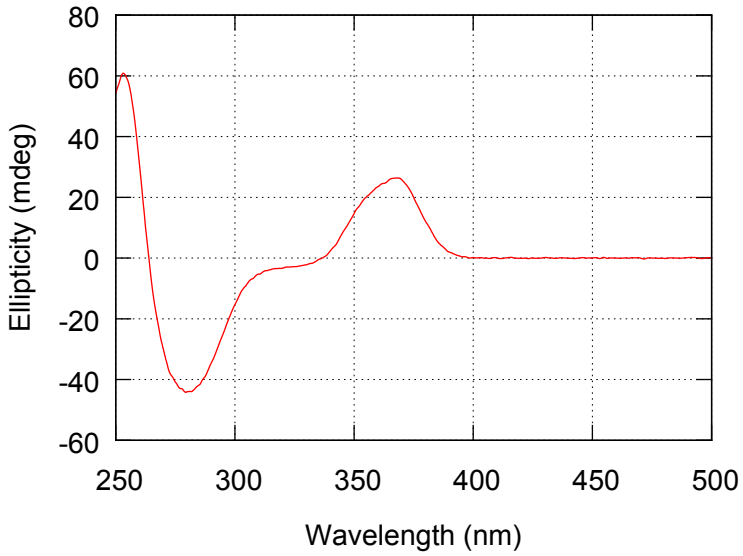

Figure S76. CD spectrum of **3(200)** in CH_2Cl_2 (2.22×10^{-2} g/L, path length = 10 mm).

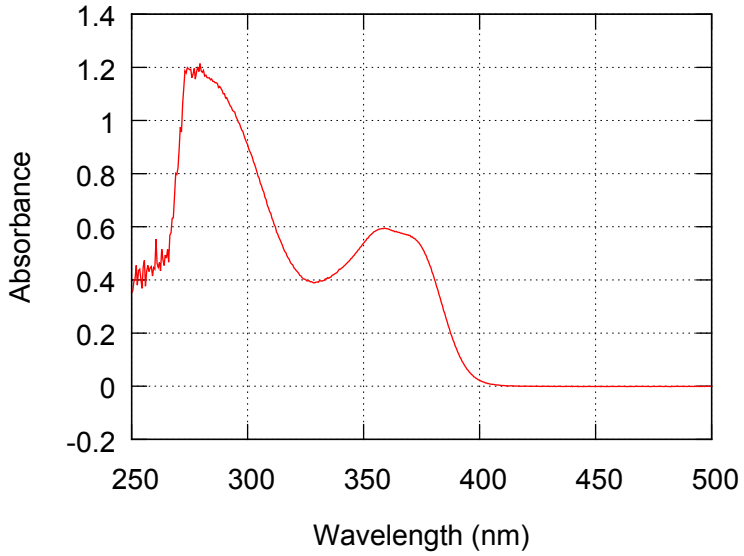

Figure S77. UV-vis absorption spectrum of **3(200)** in trichloroethylene (2.22×10^{-2} g/L, path length = 10 mm).

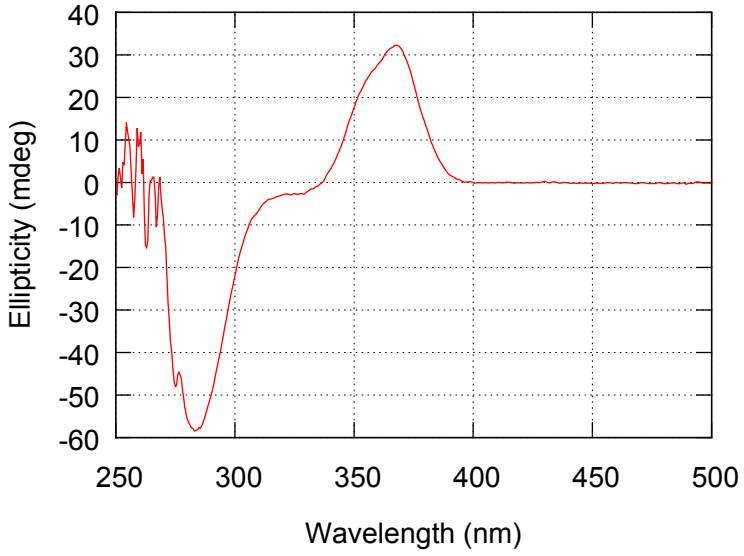

Figure S78. CD spectrum of **3(200)** in trichloroethylene (2.22×10^{-2} g/L, path length = 10 mm).

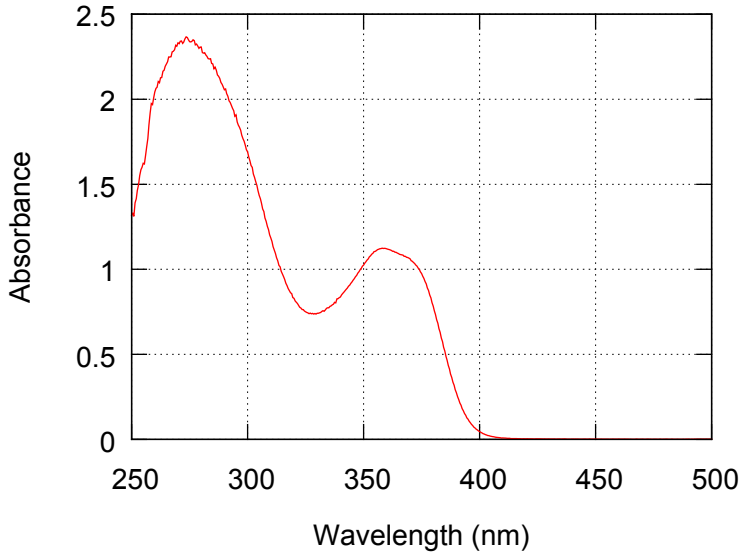

Figure S79. UV-vis absorption spectrum of **3(200)** in THF (4.44×10^{-2} g/L, path length = 10 mm).

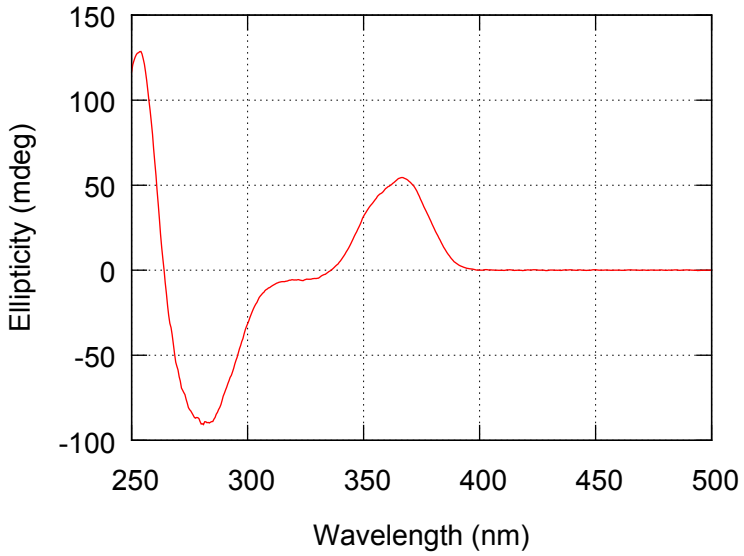

Figure S80. CD spectrum of **3(200)** in THF (4.44×10^{-2} g/L, path length = 10 mm).

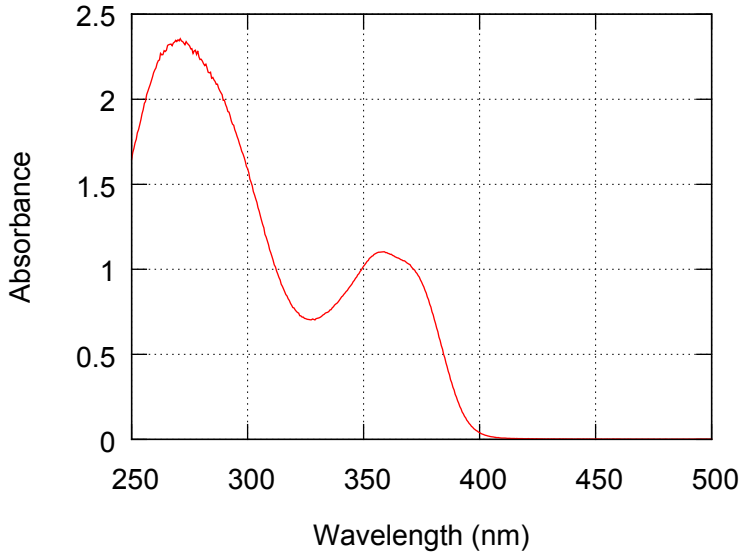

Figure S81. UV-vis absorption spectrum of **3(200)** in MTBE (4.44×10^{-2} g/L, path length = 10 mm).

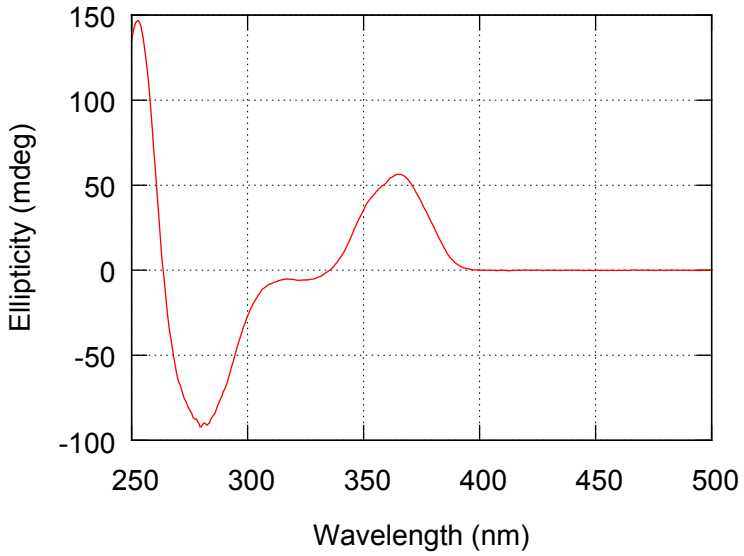

Figure S82. CD spectrum of **3(200)** in MTBE (4.44×10^{-2} g/L, path length = 10 mm).

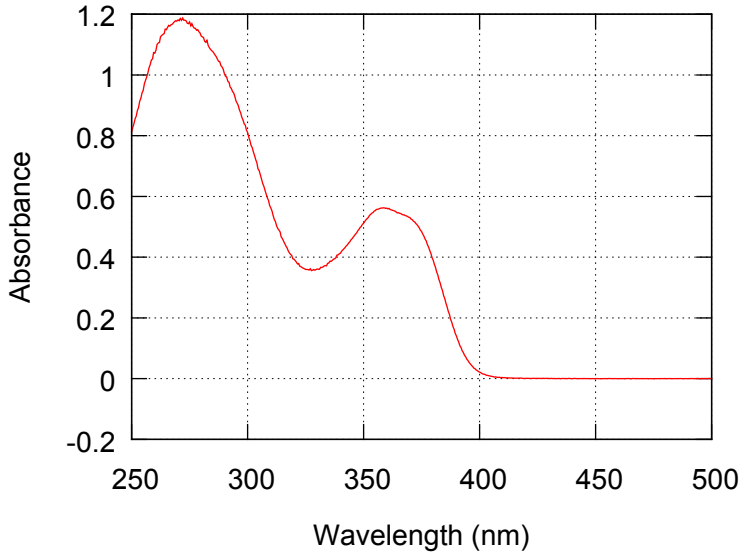

Figure S83. UV-vis absorption spectrum of **3(200)** in CPME (2.22×10^{-2} g/L, path length = 10 mm).

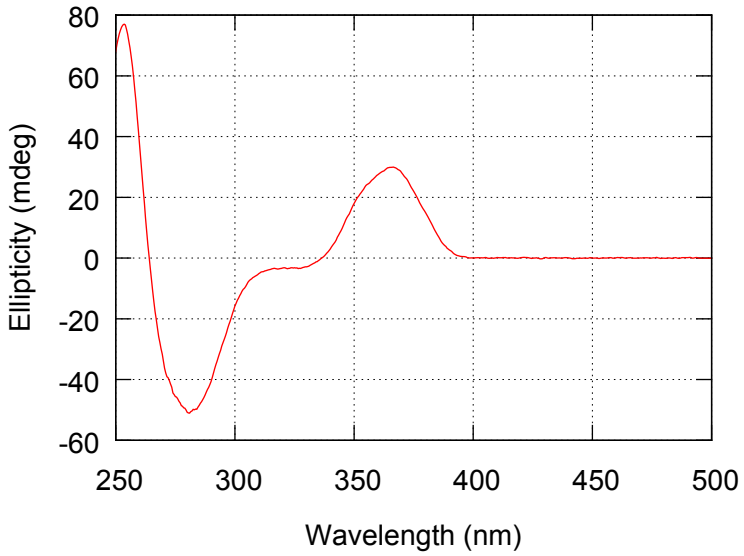

Figure S84. CD spectrum of **3(200)** in CPME (2.22×10^{-2} g/L, path length = 10 mm).

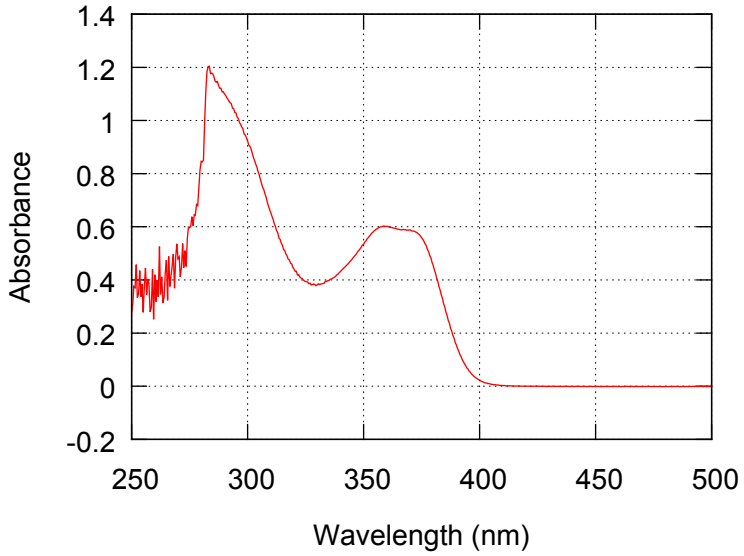

Figure S85. UV-vis absorption spectrum of **3(200)** in toluene (2.22×10^{-2} g/L, path length = 10 mm).

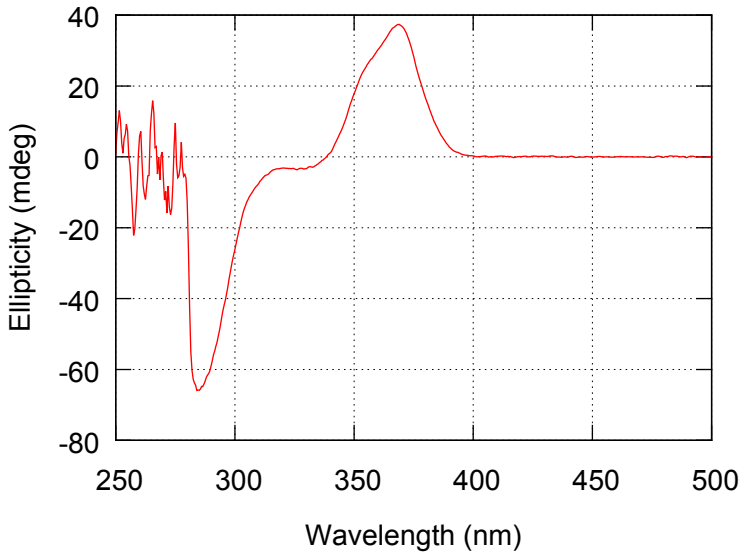

Figure S86. CD spectrum of **3(200)** in toluene (2.22×10^{-2} g/L, path length = 10 mm).

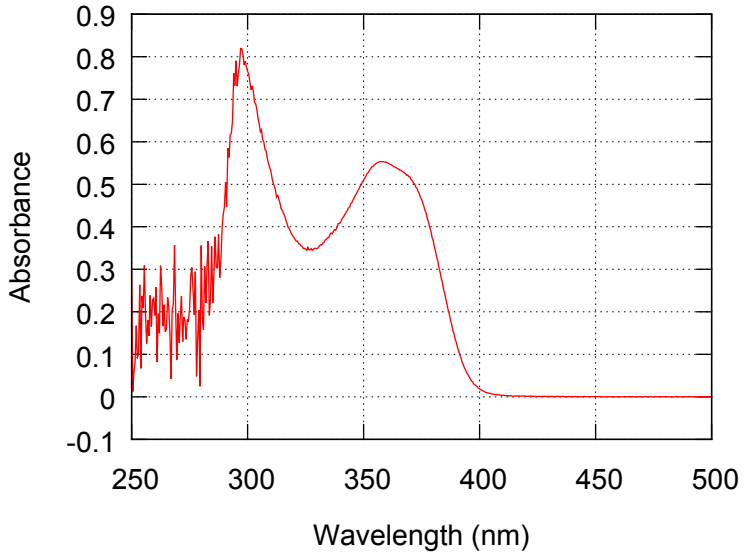

Figure S87. UV-vis absorption spectrum of **3(200)** in NEt_3 (2.22×10^{-2} g/L, path length = 10 mm).

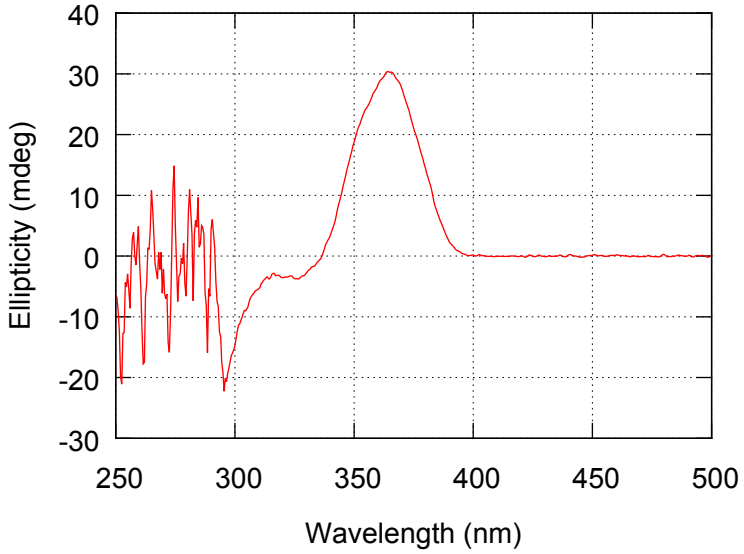

Figure S88. CD spectrum of **3(200)** in NEt_3 (2.22×10^{-2} g/L, path length = 10 mm).

3 PL Spectra of New Compounds

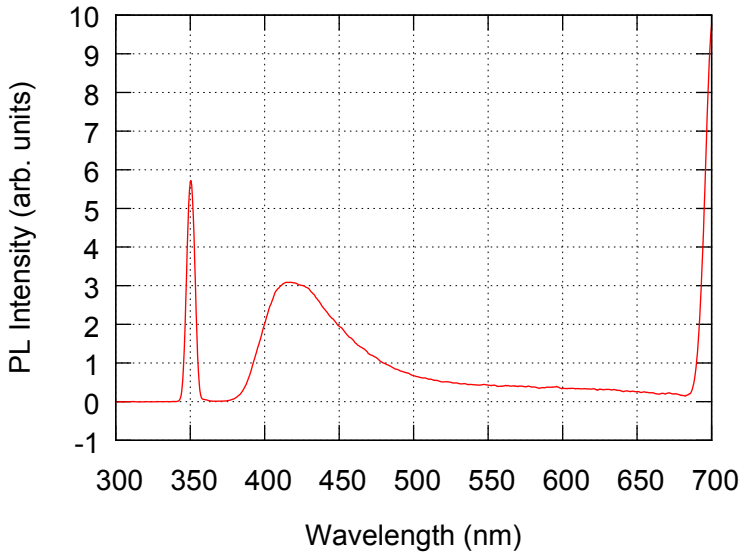

Figure S89. PL spectrum of **1(200)** in $CHCl_3$ (1.6×10^{-2} g/L, excited at 350.0 nm).

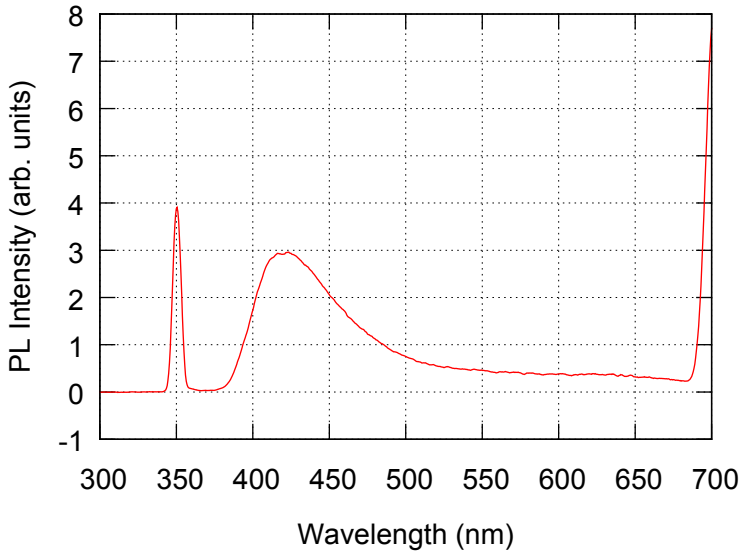

Figure S90. PL spectrum of **1(200)** in 1,1,1-TCE (1.6×10^{-2} g/L, excited at 350.0 nm).

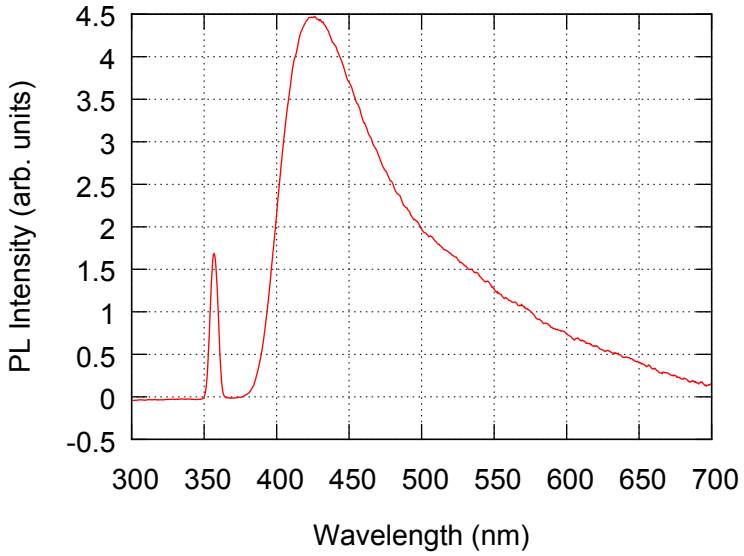

Figure S91. PL spectrum of **2(200)** in $CHCl_3$ (2.36×10^{-2} g/L, excited at 356.5 nm).

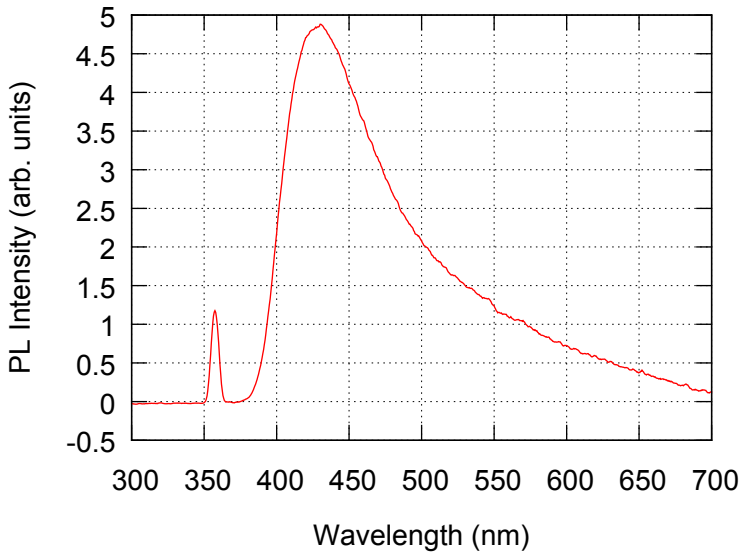

Figure S92. PL spectrum of **2(200)** in 1,1,1-TCE (2.36×10^{-2} g/L, excited at 357.0 nm).

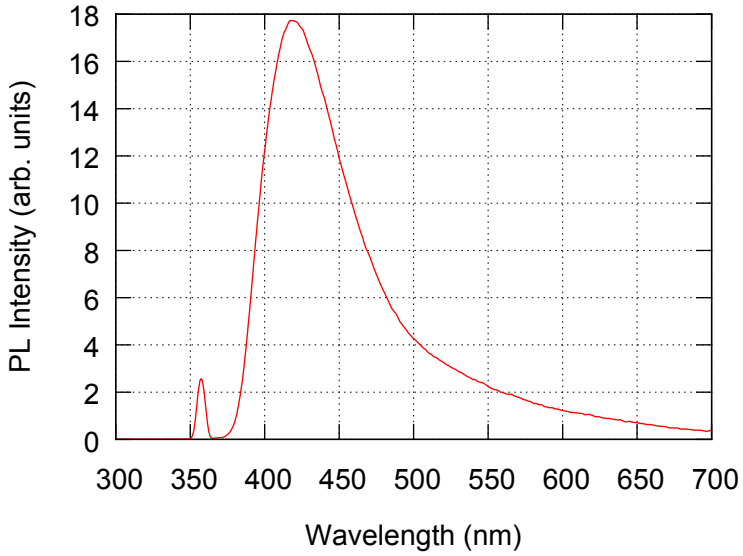

Figure S93. PL spectrum of **3(200)** in $CHCl_3$ (2.12×10^{-2} g/L, excited at 356.5 nm).

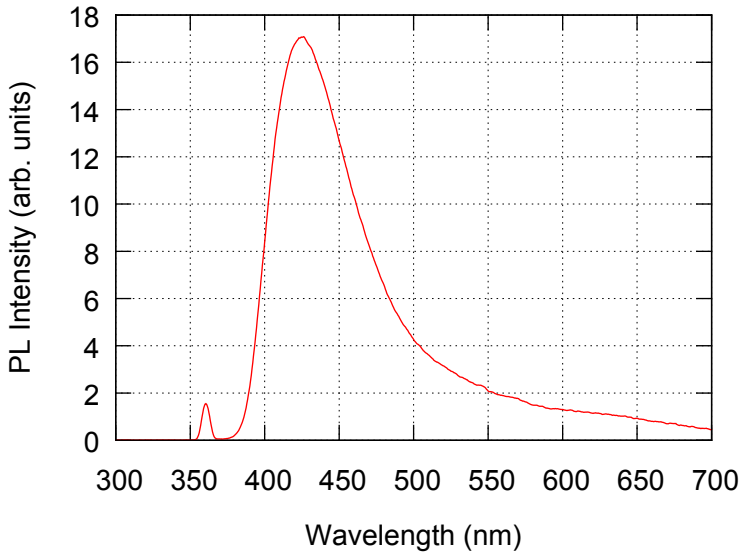

Figure S94. PL spectrum of **3(200)** in 1,1,1-TCE (2.12×10^{-2} g/L, excited at 359.5 nm).

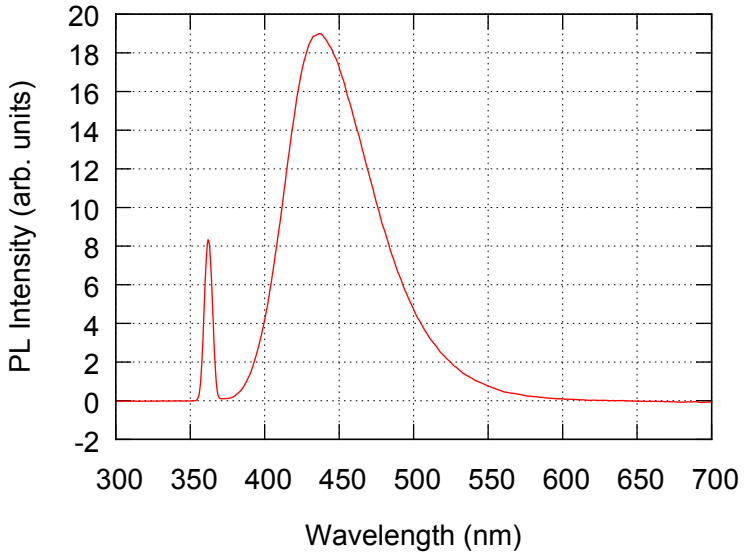

Figure S95. PL spectrum of **4** in $CHCl_3$ (4.82×10^{-3} g/L, excited at 362.0 nm).

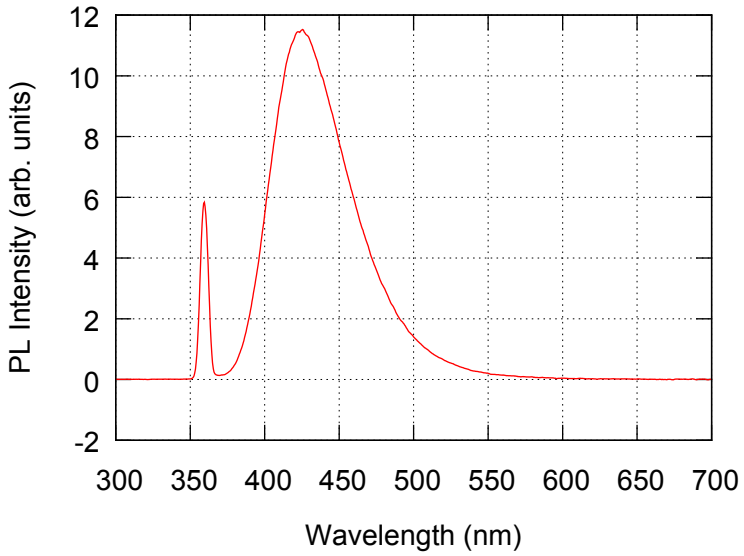

Figure S96. PL spectrum of **4** in 1,1,1-TCE (4.82×10^{-3} g/L, excited at 359.5 nm).